King's Research Portal

Link to publication record in King's Research Portal

1 # Wnt signaling regulates cytosolic translocation of Connexin

2 # 43

3 Xiaoming Hou[1,2,¶], Mohammad R A Khan[3] , Mark Turmaine[4], Christopher Thrasivoulou[2] , David L

4 Becker[2,5]and Aamir Ahmed[1,3]*

5 [1] Prostate Cancer Research Centre, 67 Riding House Street, Division of Surgery, University College

6 London, London, W1W 7EJ, United Kingdom; [2]Research Department of Cell and Developmental

7 Biology, The Centre for Cell and Molecular Dynamics, Rockefeller Building, University College

8 London, London, WC1E 6JJ, United Kingdom; [3]Prostate Cancer Research Centre at the Centre for

9 Stem Cells and Regenerative Medicine, King's College London, 28th Floor, Tower Wing, Guy's

10 Hospital, Great Maze Pond, London SE1 9RT; [4]Division of Biosciences, University College London,

11 Gower Street, London WC1E 6BT, United Kingdom; [5] Lee Kong Chian School of Medicine, Nanyang

12 Technological University, 11, Mandalay Road, Singapore, 308232: Institute of Medical Biology,

13 A*STAR, 8A- Biomedical Grove, Biopolis, Singapore 138648.

14

15

16 [¶]Current address: Department of Paediatrics, Provincial Hospital Affiliated to Shandong University,

17 Jinan, PR China

18

19 *Corresponding author: Centre for Stem Cells and Regenerative Medicine, King's College London,

20 28th Floor, Tower Wing, Guy's Hospital, Great Maze Pond, London SE1 9RT

21 Telephone: +44 207188 7188 xtn 55708

22 Email: aamir.ahmed@kcl.ac.uk

23   **Abstract**

24   The availability of intracellular, stabilized ß-catenin, a transcription factor co-activator, is tightly

25   regulated; ß-catenin is translocated into the nucleus in response to Wnt ligand binding to its cell

26   membrane receptors. Here we show that Wnt signal activation in mammalian cells activates

27   intracellular mobilization of Connexin 43 which belongs to a gap junction protein family, a new

28   target protein in response to extracellular Wnt signal activation. Transmission electron microscopy

29   (TEM) showed that the nuclear localization of Cx43 was increased by 8-10 fold in Wnt5A and 9B

30   treated cells compared to controls; this Wnt induced increase was negated in the cells where Cx43

31   and ß-catenin were knocked down using shRNA. There was a significant ($p<0.001$) and concomitant

32   depletion of the cell membrane and cytosolic signal of Cx43 in Wnt treated cells with an increase in

33   the nuclear signal for Cx43; this was more obvious in cells where β-catenin was knocked down using

34   shRNA. Conversely, Cx43 knockdown resulted in increased ß-catenin in the nucleus, in the absence

35   of Wnt activation. Co-immunoprecipitation of Cx43 and ß-catenin proteins with a casein kinase

36   (CKIδ) antibody showed that Cx43 interacts with ß-catenin and may form part of the so-called

37   destruction complex. Functionally, Wnt activation increased the rate of wound re-epithelization in

38   rat skin, *in vivo*.

39   **Introduction**

40   The Wnt signaling pathway is known to play a key role in development (e.g. bone and limb

41   morphogenesis) and disease (12), including cancer, osteoporosis and also in wound healing (54).

42   There are two major intracellular transducers of Wnt signaling CTNNB1 (cadherin associated protein

43   ß or ß-catenin, (34) and Ca^{2+} (40); ß-catenin and CTNNB1 are used interchangeably in this

44   manuscript). ß-catenin, was first discovered as a part of the adherent junction complex in the cell

45   membranes of NIH 3T3 cell line (32). Wnt ligand binding to its plasma membrane receptor complex

46   (5) activates intracellular calcium [Ca2+]i and desequesters and stabilizes ß-catenin from a multi-

47   protein complex termed the ß-catenin destruction complex (44). Subsequent to its release from the

48   destruction complex in the cytosol ß-catenin is translocated to the nucleus where it activates gene

49   transcription in conjunction with LEF/TCF proteins (4). Recent studies have shown that, in

50   mammalian cells, Ca^{2+} and ß-catenin signaling act in a coordinated, interdependent manner (48).

51   Whether Wnt signaling activation is involved in the translocation of a protein other than ß-catenin to

52   the nucleus is not known. We demonstrate that Wnt signaling activation initiates translocation of at

53   least one other protein, namely Connexin 43 (Cx43), a member of the gap junctional intercellular

54   communication (GJIC) family of proteins.

55

56   GJIC is involved in tissue homeostasis and Connexins, a family of gap junction forming proteins, are a

57   key component of GJIC. The Connexin gene family comprises of 21 members in man and 20 in mouse

58   (19 of which can be grouped as orthologous genes) that share high sequence similarity at both gene

59   and protein levels (42); GJA1 (gap junction α-1 or Cx43) is one member of the Connexin family that is

60   highly conserved in mammals (98% protein sequence identity in human and mouse protein

61   sequences) (41). Mutations in Cx43 have been associated with occulo-dentodigital dysplasia (33) and

62   autosomal recessive craniometaphyseal dysplasia (20). Cx43 is the most abundant of the Connexins

63   in skin, and is expressed in keratinocytes, fibroblasts, endothelial cells and dermal appendages (3).

64   Besides the formation of GJIC, C-terminal portion of Cx43 (CT-Cx43) was reported to localize to the

65   cytosol and nucleus of both cardiomyocytes and HeLa cells(15). Stable expression of CT-Cx43 in HeLa

66   cells induced significant gowth suppression(15). Cx43 plays a role in wound healing during which a

67   decrease in the expression of Cx43 protein is observed within the first 6-48h after injury at the

68   wound edge (3). Topical application of a Cx43-specific antisense oligodeoxynucleotide to acute

69   wounds in rodent models speeds up the wound healing process (27, 36); incidentally, a recent study

70   showed acceleration of wound healing via the activation of the Wnt signaling pathway (54).

71

72   Previous work has hinted at a relationship between Wnt signaling, particularly ß-catenin (37) and

73   Cx43 using over-expression or knockdown of Wnt signaling related proteins or Cx43. For example,

74   Cx43 is considered a target of ß-catenin transcription through the activation Wnt signaling with

75   Wnt1 (1, 30, 49); activation of Wnt signaling by Wnt3A, for 72h, also increased expression of Cx43 in

76   vascular smooth muscle cells (9); ß-catenin knockdown reduced Cx43 expression and GJIC in mouse

77   granulosa cells or osteocytes (52, 55). Furthermore, Cx43 overexpression decreased nuclear levels of

78   ß-catenin (46, 47), and reduced TCF luciferase activity in colorectal cancer and neural progenitor

79   cells (37, 39). ß-catenin level increased in conditional osteocytes or sertoli cell knockout Cx43

80   transgenic mice (6, 7), however, β-catenin expression is attenuated in Cx43 deficient fractures (23).

81   Interestingly, ß-catenin and Cx43 are thought partly to co-localize in the cell membrane (39).

82

83   Considering the key functions of Wnt signaling and the putative relationship between ß-catenin, a

84   key transducer of Wnt signaling, and Cx43, we questioned whether Wnt signal activation might

85   modulate Cx43 in mammalian cells? We show here that subsequent to Wnt signaling activation Cx43

86   is translocated into the nucleus in a similar manner to that of ß-catenin in at least two different

87   mammalian cell lines. ShRNA mediated knockdown of ß-catenin increased intracellular movement of

88   Cx43 to the nucleus and *vice versa*. Quantitation of Cx43 expression shows that the membrane and

89   cytosolic Cx43 is translocated in response to the activation of Wnt signaling and that it interacts with

90   the proteins associated with the so called ß-catenin destruction complex. We propose that there is

91   cross-talk between Wnt signaling and Cx43 and that Wnt signal activation modulates intracellular

92   Cx43 movement. We provide a new, in vitro, model for the regulation of Cx43 by Wnt signaling and

93   identify a new target protein in response to the activation of Wnt signaling.

94

95   **Materials and methods**

96   *Wnt Peptides*

97   Recombinant Wnts (5A, 9B and 10B) peptides were obtained from (R&D Systems part of Bio-Techne)

98   and were made into stock solutions (at 0.1µg/µl) in phosphate buffered saline (PBS, GIBCO). Cells

99   were treated with Wnts at concentrations described in the figure legends; controls represent

100 untreated or vehicle only treated cells.

101

102 *Cell lines*

103 Cell lines (PC3 human prostate cancer, 3T3 mouse fibroblast) were obtained through ATCC via John

104 Masters (University College London). PC3 cells were grown in RPMI 1640 (Gibco) cell culture medium

105 supplemented with 10% fetal bovine serum (FBS) and L-glutamine. 3T3 fibroblasts were grown in

106 DMEM-GlutaMAX™-1 (Gibco) supplemented with 10% FBS; cells were grown in 5% CO_2 at 37°C.

107 Human embryonic kidney (GP-293 and 293FT) cell lines were used for viral transduction and were

108 obtained from the kit manufacturer (Clontech) (25).

109

110 *Retroviral and lentiviral constructs and transduction*

111 Cx43-specific shRNA target sequence GGTGTGGCTGTCAGTGCTC (50) was a gift of W.H. Moolenaar

112 (The Netherlands Cancer Institute); a retroviral pSuper vector (OligoEngine) containing this

113 sequence, designated Cx43shRNA, was used to establish a stable knockdown of Cx43 in cell lines

114 (25); pSuper retroviral vector without Cx43shRNA was used as control. All retroviral vectors were

115 transduced into the packaging cell line GP2–293 (Clontech) as described previously (8).

116   Lentiviral vectors containing the target sequence for ß-catenin shRNA were obtained from Addgene

117   (MA) and included: pLKO.1 (catalog number, 8453), ß-catenin target (18803) and scramble shRNA

118   (1864). Lentiviral particles were produced in 293FT cells (ATCC, at 7×10^5) and the transfection

119   complex was prepared using FuGENE 6 Transfection Reagent according to the manufacturer's

120   instructions (Roche). PC3 and 3T3 cells were transduced with retrovirus or lentivirus for 2 days and

121   were selected on the basis of antibiotic resistance.

122

123   *Immunocytochemistry*

124   Immunostaining was performed in two independent laboratories with the experimenter blinded to

125   the identity of the experiments. Cells were grown in eight-well chambered glass slides (Lab Tek II,

126   Nunc) as described, previously (25, 48). The following primary antibodies were used according to the

127   manufacturer's recommendations: Cx43 (catalog number C6219, Sigma) and ß-catenin (ab22656,

128   Abcam). Secondary antibodies (Alexa 488 or 633; Molecular Probes), goat anti-mouse peroxidase

129   Fab (Abcam) and tyramide Cy3 (Perkin Elmer) with Hoechst 33342 or 4',6-diamidino-2-phenylindole

130   (DAPI, Sigma) as a nuclear counterstain were used. Secondary antibody incubation in the absence of

131   primary antibody was used as negative control. A Leica SPE confocal microscope (Leica

132   Microsystems) was used (40x, 1.25 NA objective, sometimes with a zoom of 3x) for imaging; at least

133   three images per well, from 3–5 independent experiments were acquired. Nuclear co-localization of

134   β-catenin was calculated by JACoP analysis in Image J software (38) and represented by Pearson

135   correlation coefficient. Statistical analysis was performed using Mann–Whitney U test.

136

137   *Transmission Electron Microscopy (TEM)*

138   Cells were grown on glass coverslips, treated as previously described (48), and fixed in a mixture of

139   4% formaldehyde, 0.01% glutaraldehyde in PBS, pH 7.4 for 30mins at 4°C. Primary antibodies (Cx43,

140   diluted 1:2000, Sigma or ß-catenin, diluted 1:300) were incubated at 4°C overnight followed by

141   incubation with appropriate secondary antibodies (1.4nm Gold; ab30814 or ab30812 Abcam) also at

142   4°C overnight and post-fixed in 1% glutaraldehyde in phosphate buffer. Post-fixed cells were treated

143   with HQ Silver enhancement kit (Nanoprobes) for 3 min in the dark and then 2% osmium tetraoxide

144   (in the phosphate buffer) for 10min, rinsed, and dehydrated in a series of graded alcohols followed

145   by embedding in Agar 100 resin (Agar Scientific) as an inter-medium. Sections of 80 nm thickness

146   were collected on 300 mesh copper grids and visualised using a Joel 1010 transmission electron

147   microscope (TEM). Images were recorded using a Gatan Orius camera and analyzed using Image J.

148   The levels of Cx43 and β-catenin of different conditions and positions were calculated by setting the

149   same threshold and pixel size. For some types of analysis, images were demarcated into cell

150   membrane, cytosol and nucleus and used to calculate the level of expression of proteins in the

151   demarcated organelle by manually counting the electron dense puncta for analysis. Statistical

152   analysis for significance of difference between two groups was performed using Mann–Whitney U

153   test.

154

155   *Western blotting*

156   PC3 cells (wild type, Cx43shRNA-, pSuper, pLKO.1, scramble shRNA or ß-catenin shRNA transduced)

157   were centrifuged (1500 x*g*) and cell pellets resuspended in ice-cold radioimmunoprecipitation assay

158   buffer (RIPA) buffer with phosphatase and protease inhibitors (Roche). Protein was loaded and

159   separated on a 10% sodium dodecyl sulfate-polyacrylamide gel electrophoresis (SDS-PAGE) and

160   trans-blotted to nitrocellulose membrane (Bio-Rad). The membranes were probed with two

161   different primary antibodies against: Cx43 (C6219, Sigma, diluted 1:4000) and ß-catenin (diluted

162   1:500; ab22656, Abcam). Antibodies against α-tubulin (Sigma) or Glyceraldehyde 3-phosphate

163   dehydrogenase (GAPDH, Sigma) were used as controls for protein quantitation; Horseradish

164   peroxidase (HRP)-conjugated secondary antibodies were used, and proteins were visualized using an

165   enhanced chemiluminescence (ECL) system. Semi-quantitative analysis was performed using ImageJ

166   software and statistical analysis was performed using ANOVA or t-test.

167

168   *Co-immunoprecipitation*

169   Cells were lysed using immunoprecipitation buffer (50mM Tris, 150mM NaCl, and 1%NP-40, Sigma)

170   with protease and phosphatase inhibitors to a final volume of 1ml, the lysate was centrifuged

171   (10,000 *x g* for 5 min at 4°C) and protein concentration measured using a BCA assay (Pierce). CK1δ

172   (2-4μg, sc-20709; Santa Cruz Biotechnology) or Cx43 (4μg; C6219, Sigma) antibody was added to 1-

173   2mg total protein and mixed for 1h at 4°C. Protein A agarose (Sigma) was washed with lysis buffer

174   (3x) followed by blocking beads using 1%-2% low-IgG serum for 1h in cold room shaker. Protein A

175   agarose beads (30μl) were added to cell lysate/antibody and mixed O/N, on a rotary shaker, at 4°C.

176   The beads were washed 3x in lysis buffer at 4°C and added 50μl 2x loading buffer containing β-

177   mercaptoethanol (10%) to the washed beads to elute the precipitate. Samples were loaded onto a

178   10% SDS-PAGE gel for electrophoresis to resolve the proteins and Precision Plus Protein™ Dual Color

179   Protein Standards, (Bio Rad) used as molecular weight markers. The resolved protein was

180   transferred onto a nitrocellulose membrane which was cut into strips of 250-75kDa and 70–25kDa as

181   visualized by the markers. The membrane strips were probed with the following antibodies: β-

182   catenin(1:500; ab22656, Abcam), CK1δ(1:200; sc-55553, Santa Cruz Biotechnology, Inc.) and

183   Cx43(1:4000; C8093, Sigma) and then incubated with appropriate secondary antibodies: goat anti-

184   mouse IgG-HRP (1:2000; sc-2005, Santa Cruz Biotechnology) or Goat F(ab')2 Anti-Mouse IgM mu

185   chain-HRP (1:2000; ab5930, Abcam). The signals were detected by ECL detection using ChemiDoc™

186   XRS+ System with Image Lab™ Software (Bio Rad).

187

188   *In vivo rat cutaneous wound-healing model ± Wnts*

189   All animal procedures were subject to institutional ethical review and performed under the terms of

190   a UK Home Office license. Animals were maintained according to the United Kingdom Home Office

191   Animal (Scientific procedures) Act 1986 Code of Practice and all procedures were approved in a

192   Home Office License. A sample size calculation ($\alpha = 0.05$ and $\beta = 0.05$ and difference of mean of 100)

193   indicated a minimum sample size of 12 animals (8 experimental and 4 control). The animals were

194   housed with 12 hour light – dark cycle with free access to food and water in climatically controlled

195   rooms. Male (8 week old) Sprague-Dawley rats (Harlan Laboratories) were anesthetized by

196   inhalation of 5% halothane and maintained with 1.5% halothane. Their backs were shaved and hair

197   depilatory cream applied, washed with warm water then wiped with 70% ethanol. Skin was then

198   tented and 4 full thickness excision wounds were made with a 6mm diameter punch biopsy (27). A

199   single, topical, application of Wnt5A or Wnt9B (0.2 – 0.5μg/ml) or vehicle control was delivered to

200   each independent wound in 30% Pluronic F-127 gel (Sigma). Wounds were dressed with tegaderm

201   and animals were given analgesic before recovery. They were housed individually before they were

202   humanely killed one or three days after wounding and the wound tissue harvested for further

203   analysis (51, 54). Tissue processing, sectioning and H&E staining were performed as describe before

204   (16). The extent of re-epithelialization was measured and calculated from the wound edge (where

205   the incision was made) to the tip of new growth using Image J. Statistical analysis for significant

206   difference among different groups was performed using ANOVA.

207

208   **Results**

209   *Wnt signaling activates translocation of ß-catenin and Cx43*

210   We previously showed that addition of Wnt ligands (e.g. 5A, 9B) activates the Wnt-signaling pathway

211   as measured by translocation of ß-catenin into the nucleus in PC3 and other mammalian cells (48).

212   Similar results were found in our experiments using immunocytochemistry: there was visible but low

213   expression of ß-catenin (Fig 1 A) in control, vehicle treated, cells. Addition of Wnts increased the

214   expression of ß-catenin in the cytosol and in the nucleus (Fig 1 B-C). We tested the hypothesis that

215   Cx43 may also translocate to the nucleus in response to the activation of Wnt signaling. In PC3 cell

216   line, Cx43 expression was found to be in the cell membrane (Fig 1 D) with punctate staining pattern

217   as has been observed, previously, in other cell types (25). The staining pattern of Cx43 after addition

218   of Wnt5A and 9B (0.2μg/ml), compared to control (vehicle only), PC3 cells, showed Cx43

219   translocation towards the nucleus in a manner similar to that of ß-catenin (Fig 1 E-F). These results

220   show for the first time that the activation of Wnt signaling results in the intracellular movement of

221   Cx43 towards the nucleus in addition to the established mechanism of translocation of ß-catenin

222   into the nucleus in mammalian cells. Indeed, composite images indicate a level of apparent co-

223   translocation of ß-catenin (red) and Cx43 (green) in Wnt treated PC3 cells (Fig 1) and for Wnt 10B,

224   (Supplemental Fig S1). The Wnt induced translocation of Cx43 was not limited to PC3 cell line only.

225   3T3 cells treated with Wnt9B showed similar translocation of Cx43 (Supplemental Fig S2) as that

226   observed for PC3 cells. The expression of Cx43 was visible in the nucleus of 3T3 cells after treatment

227   with Wnt9B compared to vehicle control (Supplemental Fig S2). The translocation of Cx43 was also

228   investigated using Western blots in different cell fractions (Supplemental Fig S3). These results

229   confirm the relocation of Cx43 to the nucleus in response to Wnt activation as observed using

230   conventional immunocytochemistry (Fig 1).

231

232   *Does the activation of Wnt signaling translocate Cx43 into the nucleus?*

233   In response to Wnt signaling activation, cytosolic ß-catenin is known to desequester from the

234   'destruction complex' (44) and translocate into the nucleus where it acts as an activator of

235   transcription factors to increase the expression of genes such as c-Myc, cyclin D1, FRA1 and others

236   (19, 22). Our novel observation that Cx43 also appeared relocated in PC3 cells in response to Wnt

237   signaling (e.g. Fig 1 and Supplemental Fig S3) raised the question whether Cx43, like ß-catenin, also

238   translocates into the nucleus? We used electron microscopy to investigate this, using the same

239   antibodies as those used for immunocytochemistry (Fig 1). The expression of Cx43 was observed on

240   cell membrane and in the cytoplasm in PC3 cells (Fig 2A). It is evident in the electron micrographs

241   that the majority of Cx43 signal appears inside the nucleus subsequent to Wnt signaling activation

242   with Wnt5A or 9B (Fig 2B and 2C). The expression of Cx43 was quantified using Image J from at least

243   18 micrographs for vehicle control, Wnt5A and Wnt9B treated cells. What was seen by eye was

244   confirmed by quantitation of Cx43 signal in PC3 cells (Fig 2D). We further analyzed the expression of

245   Cx43 in different part of cell (membrane, cytosol and nucleus). Wnt5A or 9B reduced the expression

246   of Cx43 both on cell membrane and in cytosol (Fig 2 E, F and G); meanwhile both Wnts increased

247   Cx43 expression in the nucleus (Fig 2H). These results indicate, not only that Wnt signaling relocates

248   Cx43 into the cytosol, but also Cx43 translocates to the nucleus in a manner that has previously been

249   shown for ß-catenin (Fig 2I). *Cx43 knockdown: Cx43 and ß-catenin expression*

250   In order to validate the role of Wnt signaling in translocating Cx43, in addition to its known target, ß-

251   catenin, and to confirm that Cx43 was indeed translocated into the nucleus in response to Wnt

252   activation, we tested the following hypotheses: (i) that down-regulation of Cx43 expression in PC3

253   cells and other cell lines should eliminate the apparent translocation of Cx43 in response to Wnt

254   signaling (ii) that as with ß-catenin, Cx43 is translocated into the cell nucleus, subsequent to the

255   activation of Wnt signaling.

256

257   We tested the above hypotheses by using PC3 cells transduced with a Cx43 short-hairpin RNA

258   (Cx43shRNA) (50) or a control plasmid only (pSuper, termed control). The efficiency of Cx43shRNA

259   knockdown was confirmed by measuring the protein levels of Cx43 by Western blotting; Cx43

260   protein expression was reduced by 80% in cells transduced with Cx43shRNA compared to control

261   plasmid only transduced cells (Supplemental Fig S4). Cx43shRNA knockdown cells were henceforth

262   termed Cx43kd and the corresponding plasmid only control cells as Cx43c.

263

264   We first validated if transduction of control plasmid affected the observed Wnt response for Cx43

265   and ß-catenin in wild type PC3 cells. Expression of Cx43 and ß-catenin was measured using

266   fluorescence immunocytochemistry as in the wild type cells (as seen in Fig 1, above) with Cx43c cells

267   ± Wnt5A or 9B (Fig 3 A-F). Control experiments demonstrate that plasmid transduction did not alter

268   Wnt mediated Cx43 or ß-catenin response as observed in the wild type cells (Fig 1). Activation of

269   Wnt signaling appeared to relocate intracellular Cx43 protein expression in Cx43c cells and

270   compared to PBS treated cells (Fig 3A) addition of Wnt5A (Fig 3B) or Wnt9B (Fig 3C) appeared to

271   translocate Cx43 protein expression. Furthermore, compared to PBS treated Cx43c cells (Fig 3D),

272 addition of Wnt ligands (5A and 9B) also induced ß-catenin translocation (Fig 3E and F) as observed

273 in wild type cells. These results also support the notion that Cx43 location is regulated by the Wnt

274 signaling pathway.

275

276 Cx43kd cells showed decreased Cx43 expression when measured using immunofluorescence (Fig

277 3G), this was also the case after Wnt5A or 9B treatment (Fig 3H and I). These results indicate that

278 Cx43 shRNA mediated knockdown reduces the protein expression of Cx43 in Cx43kd cells and

279 supports the data obtained using Western blotting (Supplemental Fig S4).

280

281 The expression and distribution of ß-catenin was also determined in Cx43kd cells treated with Wnt

282 ligands using western blot (Supplemental Fig S4) and immunofluorescence (Fig 3 J-L). The total ß-

283 catenin protein levels did not alter significantly after Cx43 knockdown measured using Western blot

284 technique, however, remarkably, the intracellular distribution of ß-catenin was changed (Fig 3J): ß-

285 catenin in the Cx43kd cells appears to be released into the cytosol with limited nuclear co-

286 localization compared to Cx43c cells (Fig 3J compared to Fig 3D and Fig 4A; co-localization of ß-

287 catenin and the nuclear stain, DAPI, was determined using Image J software as described in

288 materials and method). There was a significant increase in the co-localization coefficients of nuclear

289 co-localization of ß-catenin in Cx43kd PC3 cells (Fig 4A). Activation of Wnt signaling by Wnt5A or

290 Wnt9B in Cx43kd cells further increased the nuclear co-localization of ß-catenin compared to these

291 cells with vehicle treatment (Cx43c-vehicle treated < Cx43kd-vehicle treated < Cx43kd Wnt treated,

292 Fig 3K and L and Fig 4A). In addition to the experiments with Cx43kd in PC3 cells (above), similar

293 results were obtained in Cx43kd-3T3 cells (Fig 4B).

294

295 These results were validated using electron microscopy (Fig 5) with observations similar to those

296 obtained using immunofluorescence (Fig 3). Compared with vehicle controls (Fig 5A), the nuclear

297 Cx43 expression was increased, significantly, in Cx43c cells treated with Wnts 5A and 9B (Fig 5B-C).

298   The amount of nuclear Cx43 expression was drastically reduced in all groups of Cx43kd cell (Fig 5D-

299   G), whether or not these were treated with Wnts.

300

301   ß-catenin expression was also determined in Cx43kd and Cx43c PC3 cells ± Wnts using TEM (Fig 5H-

302   N); the signal for ß-catenin was increased in Cx43kdshRNA cells relative to Cx43c cells (Fig 5H and K).

303   Subsequent to the activation of Wnt signaling the nuclear expression of ß-catenin was increased

304   significantly ($p<0.001$) in Cx43kd cells (Fig 5L-N) compared to the cells with vehicle treatment (Fig

305   5K). These results indicate that the decrease in the expression of Cx43 leads to ß-catenin

306   displacement in the nucleus without the activation of Wnt signaling and that this process appears to

307   be enhanced after Wnt treatment.

308

309   *ß-Catenin knockdown: Cx43 and ß-catenin expression*

310   To address whether Cx43 distribution was also altered after downregulation of ß-catenin protein we

311   transduced PC3 cells with a ß-catenin short-hairpin RNA (ß-catenin (CTNNB1) shRNA, termed

312   CTNNB1kd) (31) to reduce ß-catenin protein expression; scrambled shRNA (CTNNB1sc) or a plasmid

313   (pLKO.1) only (termed CTNNB1c) transduced cells were used as controls. The efficiency of ß-catenin

314   shRNA knockdown was confirmed by Western blotting. Cells transduced with ß-catenin shRNA

315   showed reduced protein expression (around 80%) compared to CTNNB1sc or CTNNB1c

316   (Supplemental Fig S4). Incidentally, no significant difference was observed in the total Cx43 protein

317   level after CTNNB1 knockdown in Western blots (Supplemental Fig S4).

318

319   Immunofluorescence was used to establish that Wnt response in CTNNB1sc or CTNNB1c was not

320   altered for ß-catenin or Cx43 expression and regulation. Expression of ß-catenin was visible in the

321   nucleus of CTNNB1sc or CTNNB1c cells treated with Wnt5A and Wnt9B compared to the cells that

322   were treated with vehicle control (Fig 6A-C and G-I). The quantified data is given in Fig 4C. Similar

323   results were obtained for Cx43 expression in response to Wnt activation (Fig 6D-F and J-L). These

324   results indicate that viral transduction did not cause a change in Wnt mediated ß-catenin or Cx43

325   response as observed in the wild type cells (Fig 1).

326

327   CTNNB1kd cells also showed decreased ß-catenin expression using immunofluorescence (Fig 6M),

328   this was also the case even after Wnt treatment (Fig 6N and O). The apparent cellular distribution of

329   Cx43 was different to that observed in CTNNB1c, CTNNB1sc (Fig 6D and J) or wild type cells (Fig 1).

330   There was little Cx43 in the nucleus in CTNNB1c and CTNNB1sc cells (Fig 6D and J), but Cx43 was

331   found in nucleus of CTNNB1kd PC3 cells (Fig 6P); addition of Wnt5A and Wnt9B in CTNNB1kd PC3

332   cells induced further Cx43 protein to translocate to nucleus compared to vehicle treated cells (Fig 6Q

333   and R).

334

335   To further confirm these observations, Cx43 expression was determined in CTNNB1kd cells,

336   CTNNB1c and CTNNB1sc cells in response to Wnts by TEM (Fig 7). Cx43 expression was calculated as

337   expression / nucleus from multiple micrographs. Relative to CTNNB1c and CTNNB1sc cells the

338   nuclear expression of Cx43 was increased in CTNNB1kd cells (Fig 7A, D and G). Also, compared to

339   vehicle treated CTNNB1kd PC3 cells (Fig 7G), cells treated with Wnts 5A or 9B showed an increased

340   nuclear expression of Cx43 (Fig 7H and I). These results indicate that β-catenin knockdown leads to

341   Cx43 translocation to nucleus and this translocation increased in response to Wnt signaling

342   activation.

343

344   *Cx43 is a likely partner in the ß-catenin destruction complex*

345   To examine whether Cx43 was a component of the so called destruction complex (44) we used co-

346   immunoprecipitation technique with β-catenin and CK1 δ (part of the destruction complex proteins),

347   to investigate if Cx43 interacts with the two destruction complex proteins in PC3 cells. We found that

348   both β-catenin and Cx43 were in native CK1δ complexes from PC3 cells (Fig 8). Furthermore, β-

349   catenin and CK1δ were also detected in Cx43 complexes (Fig 8). These results indicate that Cx43,

350   CK1δ and β-catenin interacts with each other in PC3 cells and Cx43 may be a component of the

351   destruction complex.

352

353   *Accelerated re-epithelialization in Wnt ligand-treated wounds in vivo*

354   A reduction in Cx43 protein expression plays a key role in the wound healing process (3). If Wnt

355   signaling regulates Cx43 *in vitro*, as seen by the experiments described above, can Wnt mediated

356   translocation of Cx43 from *in vivo* woun*d*s show similar therapeutic effects on reepithelialisation

357   rates? Having observed that Wnt signal activation accelerates fibroblast cell migration, we next

358   assessed addition of Wnts improved wound healing, *in vivo*, with a gel containing Wnts 5A and 9B,

359   applied to the wound at the time of injury (25). Wnt5A or Wnt9B treatment accelerated the rate of

360   re-epithelialization compared to control rats at 1 day after wounding (Fig 9A-C and G). The

361   significantly increased rate of re-epithelialization, following Wnt5A or 9B treatment, disappeared at

362   3 days after wounding (Fig 9D-F and G). These results indicated that activation of Wnt signaling has

363   significant effects *in vivo*, similar to those observed for Cx43 knockdown in previous studies (36).

364

365   **Discussion**

366   The mechanism of Wnt signaling has been conventionally thought to be via two distinct pathways

367   the Wnt/ β-Catenin (canonical) and Wnt / Ca^{2+} (non-canonical) (29). In this report, we demonstrate,

368   for the first time, that Wnt signal activation, in addition to the well-established activation of

369   intracellular calcium and translocation of ß-catenin into the nucleus, also leads to the translocation

370   of Cx43 to the nucleus, in mammalian cell lines. Immunostaining, both using fluorescence and TEM,

371   showed Cx43 protein behaves in a similar manner to ß-catenin in response to the activation of Wnt

372   signaling.

373   Cx43 is best known as a key component of GJIC on the membrane (3, 28) and much research in this

374   field is directed towards understanding the role Cx43 plays in GJIC. For example, in cardiomyocytes

375   and HeLa cells the C-terminal portion of Cx43 (CT-Cx43) is reported to be localized in the cytosol and

376   nucleus (15). Our results demonstrate that it is the membrane and possibly cytosolic Cx43 that

377   appears, largely, to be translocated into the nucleus subsequent to Wnt signaling activation. These

378   results were validated as the cytosolic/membrane Cx43 signal and its translocation to the nucleus

379   after Wnt activation, were almost completely abolished in cells knocked down for Cx43 in both PC3

380   and 3T3 cells.

381

382   *Nuclear expression of Cx43*

383   Cx43 contains a nuclear targeting sequence in its C-terminal domain (35, 58) and therefore its

384   presence in the nucleus is not surprising. This occurs for both, the whole, or partial (C-terminus),

385   acetylated or phosphorylated Cx43 protein (10, 11, 13-15, 17, 18, 21, 24, 26, 56, 57). There are other

386   structural clues as to why Cx43 expression is often found in the nucleus. For example,

387   immunoprecipitation and mass spectrometric analysis suggests that Cx43 interacts with two

388   components of the nuclear translocation system: the GTP-binding nuclear protein Ran (RAN) and

389   importin (KPNB1)(18). Furthermore, by using cNLS (nuclear localization signal) Mapper the C-

390   terminal tail of Cx43 has been shown to contain two potential NLSs that are recognized by the

391   importin α/β complex, which imports proteins to the nucleus through the RAN-GTP cycle (18). Also,

392   many Cx43-nuclear interactors have been identified, including several histones, transcription factors

393   and nucleolar proteins, such as nucleolin or the polymerase I and transcript release factor (PTRF).

394   This suggests that Cx43 or its C-terminal tail might affect chromatin organization, nucleolar activity,

395   rRNA transcription and termination (18). During cell cycle progression of A549 lung cancer cell lines,

396   Cx43 is translocated to the nucleus via A-kinase anchoring protein 95 (AKAP95) in late G1 phase. In

397   the nucleus, Cx43-AKAP95 protein complex simultaneously binds DNA and this co-localization

398   implies that Cx43 regulate DNA expression or participate in DNA aggregation and condensation (11).

399   Functionally, nuclear localization of Cx43 has been co-related to slower growth (26), cell cycle

400   progression (11), apoptosis induction (24, 56, 57), activation of gene transcription (13, 18), or tumor

401   formation (14, 17, 21). The extracellular signals that modulate have not been greatly elucidated.

402 Previous studies have shown that Wnt treatment (with Wnt1 or Wnt3A) for at least 24h or even

403 longer increased the expression of Cx43 and promoted intercellular communication in several cell

404 lines (1, 30, 49). Our investigations demonstrate an effect of Wnt activation on Cx43 in a shorter

405 time span (within minutes), similar to that observed for the documented translocation of Wnt

406 mediated ß-catenin translocation (48).

407

408 *Where is Cx43 translocated from in response to Wnt signal activation?*

409 Estimates from our electron micrographs (Fig 2) show that the range of distribution of Cx43 signal

410 within wild type cells is 10-20%, 20-50% and 5-10% in the cell membrane, cytosol and nucleus,

411 respectively (Fig 2E, F and G). Activation of Wnt signaling results in the re-distribution of Cx43 signal

412 as follows: 5-10%, 10-20% and 50-60% in the cell membrane, cytosol and nucleus, respectively (Fig

413 2E, F and G). It must be emphasized that these are estimates, based on TEM, and may not reflect the

414 true total distribution of Cx43 within PC3 cells. If, however, the assumptions hold and this is the

415 'normal' distribution of Cx43 in these cell lines, it would indicate that the majority of Wnt mediated

416 translocation of Cx43 occurs from the cytosolic pool.

417

418 *Cx43 expression and ß-catenin, localization and translocation in response to Wnts*

419   A major extracellular signal for nuclear translocation for Cx43 appears to be extracellular Wnt signal

420 activation. The Wnt signaling pathway is well established as an activator of intracellular ß-catenin

421 translocation into the nucleus. A surprising observation in our study was the apparent relocation of

422 ß-catenin due to Cx43 knockdown (Fig 3J-L, Fig 4 and Fig 5H-N). This observation is complementary

423 to previous studies in which over-expression of Cx43 was reported to show a decrease in the nuclear

424 levels of ß-catenin (46, 47) and reduced TCF luciferase activity in colorectal cancer and neural

425 progenitor cells (37, 39). Conversely, knockdown of β-catenin appears to alter the spatial distribution

426 of Cx43 in PC3 cells. There have been suggestions, sometimes contradictory (6, 7, 23, 52, 55), that

427 knockdown of either Cx43 or ß-catenin alters the expression of the other. We did not observe

428 alterations in the expression levels of Cx43 or ß-catenin in either PC3 or 3T3 cells that some previous

429 studies suggested (6, 7, 23, 52, 55). This suggests a structural link between intracellular ß-catenin

430 and Cx43 proteins.

431

432 Considering that ß-catenin and Cx43 are thought partly to co-localize on the cell membrane (39) and

433 some researchers found that β-catenin appeared to be sequestrated by Cx43 as part of a complex

434 within the junctional membrane (2, 6, 37, 47), these two proteins (ß-catenin and Cx43) may share a

435 closer relationship than expected or reported, previously. Our data add significant weight to this

436 notion, by demonstrating a direct co-relation between the Wnt signaling pathway that regulates the

437 topographical location of ß-catenin and Cx43. These results suggest for the first time, that the two

438 proteins exerting a caging effect upon each other– similar to that of the destruction complex on

439 intracellular ß-catenin (44). And our results indicate that Cx43 may be a component of the

440 destruction complex (Fig 8). The overall impact of ß-catenin and Cx43 appears to be a brake on the

441 displacement of each other under normal conditions whilst moving concomitantly in response to

442 Wnt signal activation.

443

444 The results from this study showed that Wnts reduced the expression of Cx43 on the membrane and

445 the cytosol and promoted the translocation of Cx43 into the nucleus. We applied the Wnt5A and 9B

446 ligands to full thickness skin wounds in rats and discovered that Wnt signaling increased the rate of

447 wound healing *in vivo*. As with gene transcription, we observed an impact of Cx43 expression in the

448 migratory capabilities of mammalian cells, *in vitro* (Supplemental Fig S5) *and in vivo* (Fig 9).

449

450 We propose a new model (Fig 10) in which activation of Wnt signaling by Wnt ligand / receptor

451 binding activates not only desequestration and translocation of ß-catenin from the destruction

452 complex into the nucleus, as is well known (43), but also release and translocate Cx43 from the

453 membrane and cytosolic compartments into the nucleus.

454

455 **Perspectives and significance**

456 This is the first demonstration of Wnt translocating another protein, other than ß-catenin indicating

457 that Wnt signaling, an evolutionarily conserved signal transduction pathway, may be regulating the

458 topography and the movement of membrane or cytosolic proteins other than the well documented

459 ß-catenin. These results provide a novel mechanism of regulation of a clinically significant

460 cytoskeletal component by a critical cell signaling pathway. This study further demonstrates, for the

461 first time, that Wnt signaling activation translocates Cx43 not just in the cytosol but into the nucleus.

462 Our research provides a novel link between two key areas of cell biology and demonstrates a unique

463 cross talk between these important cell function regulators.

464

472 **References**

473 1.   **Ai Z, Fischer A, Spray DC, Brown AM, and Fishman GI.** Wnt-1 regulation of connexin43 in
474 cardiac myocytes. *J Clin Invest* 105: 161-171, 2000.
475 2.   **Ale-Agha N, Galban S, Sobieroy C, Abdelmohsen K, Gorospe M, Sies H, and Klotz LO.** HuR
476 regulates gap junctional intercellular communication by controlling beta-catenin levels and adherens
477 junction integrity. *Hepatology* 50: 1567-1576, 2009.

478   3.   **Becker DL, Thrasivoulou C, and Phillips AR.** Connexins in wound healing; perspectives in

479   diabetic patients. *Biochim Biophys Acta* 1818: 2068-2075, 2012.

480   4.   **Behrens J, von Kries JP, Kuhl M, Bruhn L, Wedlich D, Grosschedl R, and Birchmeier W.**

481   Functional interaction of beta-catenin with the transcription factor LEF-1. *Nature* 382: 638-642,

482   1996.

483   5.   **Bhanot P, Brink M, Samos CH, Hsieh JC, Wang Y, Macke JP, Andrew D, Nathans J, and**

484   **Nusse R.** A new member of the frizzled family from Drosophila functions as a Wingless receptor.

485   *Nature* 382: 225-230, 1996.

486   6.   **Bivi N, Pacheco-Costa R, Brun LR, Murphy TR, Farlow NR, Robling AG, Bellido T, and Plotkin**

487   **LI.** Absence of Cx43 selectively from osteocytes enhances responsiveness to mechanical force in

488   mice. *J Orthop Res* 31: 1075-1081, 2013.

489   7.   **Carette D, Weider K, Gilleron J, Giese S, Dompierre J, Bergmann M, Brehm R, Denizot JP,**

490   **Segretain D, and Pointis G.** Major involvement of connexin 43 in seminiferous epithelial junction

491   dynamics and male fertility. *Dev Biol* 346: 54-67, 2010.

492   8.   **Carr AJ and Whitmore D.** Imaging of single light-responsive clock cells reveals fluctuating

493   free-running periods. *Nat Cell Biol* 7: 319-321, 2005.

494   9.   **Carthy JM, Luo Z, and McManus BM.** WNT3A induces a contractile and secretory phenotype

495   in cultured vascular smooth muscle cells that is associated with increased gap junction

496   communication. *Lab Invest* 92: 246-255, 2012.

497   10.   **Chen SC, Pelletier DB, Ao P, and Boynton AL.** Connexin43 reverses the phenotype of

498   transformed cells and alters their expression of cyclin/cyclin-dependent kinases. *Cell growth &*

499   *differentiation : the molecular biology journal of the American Association for Cancer Research* 6:

500   681-690, 1995.

501   11.   **Chen X, Kong X, Zhuang W, Teng B, Yu X, Hua S, Wang S, Liang F, Ma D, Zhang S, Zou X, Dai**

502   **Y, Yang W, and Zhang Y.** Dynamic changes in protein interaction between AKAP95 and Cx43 during

503   cell cycle progression of A549 cells. *Scientific reports* 6: 21224, 2016.

504   12.   **Clevers H and Nusse R.** Wnt/beta-catenin signaling and disease. *Cell* 149: 1192-1205, 2012.

505   13.   **Colussi C, Rosati J, Straino S, Spallotta F, Berni R, Stilli D, Rossi S, Musso E, Macchi E, Mai A,**

506   **Sbardella G, Castellano S, Chimenti C, Frustaci A, Nebbioso A, Altucci L, Capogrossi MC, and**

507   **Gaetano C.** Nepsilon-lysine acetylation determines dissociation from GAP junctions and

508   lateralization of connexin 43 in normal and dystrophic heart. *Proc Natl Acad Sci U S A* 108: 2795-

509   2800, 2011.

510   14.   **Crespin S, Fromont G, Wager M, Levillain P, Cronier L, Monvoisin A, Defamie N, and Mesnil**

511   **M.** Expression of a gap junction protein, connexin43, in a large panel of human gliomas: new

512   insights. *Cancer medicine* 5: 1742-1752, 2016.

513   15.   **Dang X, Doble BW, and Kardami E.** The carboxy-tail of connexin-43 localizes to the nucleus

514   and inhibits cell growth. *Mol Cell Biochem* 242: 35-38, 2003.

515   16.   **Davis NG, Phillips A, and Becker DL.** Connexin dynamics in the privileged wound healing of
516   the buccal mucosa. *WoundRepair Regen* 21: 571-578, 2013.
517   17.   **de Feijter AW, Matesic DF, Ruch RJ, Guan X, Chang CC, and Trosko JE.** Localization and
518   function of the connexin 43 gap-junction protein in normal and various oncogene-expressing rat liver
519   epithelial cells. *Molecular carcinogenesis* 16: 203-212, 1996.
520   18.   **Gago-Fuentes R, Fernandez-Puente P, Megias D, Carpintero-Fernandez P, Mateos J, Acea B,
521   Fonseca E, Blanco FJ, and Mayan MD.** Proteomic Analysis of Connexin 43 Reveals Novel Interactors
522   Related to Osteoarthritis. *Molecular & cellular proteomics : MCP* 14: 1831-1845, 2015.
523   19.   **Heo JS, Lee SY, and Lee JC.** Wnt/beta-catenin signaling enhances osteoblastogenic
524   differentiation from human periodontal ligament fibroblasts. *Mol Cells* 30: 449-454, 2010.
525   20.   **Hu Y, Chen IP, de AS, Tiziani V, Do Amaral CM, Gowrishankar K, Passos-Bueno MR, and
526   Reichenberger EJ.** A novel autosomal recessive GJA1 missense mutation linked to
527   Craniometaphyseal dysplasia. *PLoSOne* 8: e73576, 2013.
528   21.   **Huang RP, Fan Y, Hossain MZ, Peng A, Zeng ZL, and Boynton AL.** Reversion of the neoplastic
529   phenotype of human glioblastoma cells by connexin 43 (cx43). *Cancer Res* 58: 5089-5096, 1998.
530   22.   **Huelsken J and Behrens J.** The Wnt signalling pathway. *JCell Sci* 115: 3977-3978, 2002.
531   23.   **Loiselle AE, Lloyd SA, Paul EM, Lewis GS, and Donahue HJ.** Inhibition of GSK-3beta rescues
532   the impairments in bone formation and mechanical properties associated with fracture healing in
533   osteoblast selective connexin 43 deficient mice. *PLoS ONE* 8: e81399, 2013.
534   24.   **Mauro V, Carette D, Pontier-Bres R, Dompierre J, Czerucka D, Segretain D, Gilleron J, and
535   Pointis G.** The anti-mitotic drug griseofulvin induces apoptosis of human germ cell tumor cells
536   through a connexin 43-dependent molecular mechanism. *Apoptosis : an international journal on
537   programmed cell death* 18: 480-491, 2013.
538   25.   **Mendoza-Naranjo A, Cormie P, Serrano AE, Hu R, O'Neill S, Wang CM, Thrasivoulou C,
539   Power KT, White A, Serena T, Phillips AR, and Becker DL.** Targeting Cx43 and N-cadherin, which are
540   abnormally upregulated in venous leg ulcers, influences migration, adhesion and activation of Rho
541   GTPases. *PLoS ONE* 7: e37374, 2012.
542   26.   **Mennecier G, Derangeon M, Coronas V, Herve JC, and Mesnil M.** Aberrant expression and
543   localization of connexin43 and connexin30 in a rat glioma cell line. *Molecular carcinogenesis* 47: 391-
544   401, 2008.
545   27.   **Mori R, Power KT, Wang CM, Martin P, and Becker DL.** Acute downregulation of connexin43
546   at wound sites leads to a reduced inflammatory response, enhanced keratinocyte proliferation and
547   wound fibroblast migration. *J Cell Sci* 119: 5193-5203, 2006.
548   28.   **Nielsen MS, Axelsen LN, Sorgen PL, Verma V, Delmar M, and Holstein-Rathlou NH.** Gap
549   junctions. *Compr Physiol* 2: 1981-2035, 2012.
550   29.   **Nusse R.** Wnt signaling. *Cold Spring HarbPerspectBiol* 4: pii: a011163, 2012.
551   30.   **Olson DJ, Christian JL, and Moon RT.** Effect of wnt-1 and related proteins on gap junctional
552   communication in Xenopus embryos. *Science* 252: 1173-1176, 1991.

553   31.   **Onder TT, Gupta PB, Mani SA, Yang J, Lander ES, and Weinberg RA.** Loss of E-cadherin
554   promotes metastasis via multiple downstream transcriptional pathways. *Cancer Res* 68: 3645-3654,
555   2008.

556   32.   **Ozawa M, Baribault H, and Kemler R.** The cytoplasmic domain of the cell adhesion molecule
557   uvomorulin associates with three independent proteins structurally related in different species.
558   *EMBO J* 8: 1711-1717, 1989.

559   33.   **Paznekas WA, Boyadjiev SA, Shapiro RE, Daniels O, Wollnik B, Keegan CE, Innis JW, Dinulos
560   MB, Christian C, Hannibal MC, and Jabs EW.** Connexin 43 (GJA1) mutations cause the pleiotropic
561   phenotype of oculodentodigital dysplasia. *AmJHumGenet* 72: 408-418, 2003.

562   34.   **Peifer M, McCrea PD, Green KJ, Wieschaus E, and Gumbiner BM.** The vertebrate adhesive
563   junction proteins beta-catenin and plakoglobin and the Drosophila segment polarity gene armadillo
564   form a multigene family with similar properties. *J Cell Biol* 118: 681-691, 1992.

565   35.   **Qin H, Shao Q, Curtis H, Galipeau J, Belliveau DJ, Wang T, Alaoui-Jamali MA, and Laird DW.**
566   Retroviral delivery of connexin genes to human breast tumor cells inhibits in vivo tumor growth by a
567   mechanism that is independent of significant gap junctional intercellular communication. *J Biol Chem*
568   277: 29132-29138, 2002.

569   36.   **Qiu C, Coutinho P, Frank S, Franke S, Law LY, Martin P, Green CR, and Becker DL.** Targeting
570   connexin43 expression accelerates the rate of wound repair. *Curr Biol* 13: 1697-1703, 2003.

571   37.   **Rinaldi F, Hartfield EM, Crompton LA, Badger JL, Glover CP, Kelly CM, Rosser AE, Uney JB,
572   and Caldwell MA.** Cross-regulation of Connexin43 and beta-catenin influences differentiation of
573   human neural progenitor cells. *Cell Death Dis* 5: e1017, 2014.

574   38.   **Schindelin J, Arganda-Carreras I, Frise E, Kaynig V, Longair M, Pietzsch T, Preibisch S,
575   Rueden C, Saalfeld S, Schmid B, Tinevez JY, White DJ, Hartenstein V, Eliceiri K, Tomancak P, and
576   Cardona A.** Fiji: an open-source platform for biological-image analysis. *NatMethods* 9: 676-682,
577   2012.

578   39.   **Sirnes S, Bruun J, Kolberg M, Kjenseth A, Lind GE, Svindland A, Brech A, Nesbakken A,
579   Lothe RA, Leithe E, and Rivedal E.** Connexin43 acts as a colorectal cancer tumor suppressor and
580   predicts disease outcome. *Int J Cancer* 131: 570-581, 2012.

581   40.   **Slusarski DC, Yang-Snyder J, Busa WB, and Moon RT.** Modulation of embryonic intracellular
582   Ca^{2+} signaling by Wnt-5A. *DevBiol* 182: 114-120, 1997.

583   41.   **Sohl G and Willecke K.** Gap junctions and the connexin protein family. *CardiovascRes* 62:
584   228-232, 2004.

585   42.   **Sohl G and Willecke K.** An update on connexin genes and their nomenclature in mouse and
586   man. *Cell CommunAdhes* 10: 173-180, 2003.

587   43.   **Stamos JL and Weis WI.** The beta-catenin destruction complex. *Cold Spring HarbPerspectBiol*
588   5: a007898, 2013.

589   44.   **Suh EK and Gumbiner BM.** Translocation of beta-catenin into the nucleus independent of
590   interactions with FG-rich nucleoporins. *ExpCell Res* 290: 447-456, 2003.

591   45.   **Sutcliffe JE, Chin KY, Thrasivoulou C, Serena TE, O'Neil S, Hu R, White AM, Madden L,**

592   **Richards T, Phillips AR, and Becker DL.** Abnormal connexin expression in human chronic wounds.

593   *The British journal of dermatology* 173: 1205-1215, 2015.

594   46.   **Talhouk RS, Fares MB, Rahme GJ, Hariri HH, Rayess T, Dbouk HA, Bazzoun D, Al-Labban D,**

595   **and El-Sabban ME.** Context dependent reversion of tumor phenotype by connexin-43 expression in

596   MDA-MB231 cells and MCF-7 cells: role of beta-catenin/connexin43 association. *Exp Cell Res* 319:

597   3065-3080, 2013.

598   47.   **Talhouk RS, Mroue R, Mokalled M, Abi-Mosleh L, Nehme R, Ismail A, Khalil A, Zaatari M,**

599   **and El-Sabban ME.** Heterocellular interaction enhances recruitment of alpha and beta-catenins and

600   ZO-2 into functional gap-junction complexes and induces gap junction-dependant differentiation of

601   mammary epithelial cells. *Exp Cell Res* 314: 3275-3291, 2008.

602   48.   **Thrasivoulou C, Millar M, and Ahmed A.** Activation of intracellular calcium by multiple Wnt

603   ligands and translocation of beta-catenin into the nucleus: a convergent model of Wnt/Ca2+ and

604   Wnt/beta-catenin pathways. *J Biol Chem* 288: 35651-35659, 2013.

605   49.   **van der Heyden MA, Rook MB, Hermans MM, Rijksen G, Boonstra J, Defize LH, and Destree**

606   **OH.** Identification of connexin43 as a functional target for Wnt signalling. *J Cell Sci* 111 (Pt 12): 1741-

607   1749, 1998.

608   50.   **van Zeijl L, Ponsioen B, Giepmans BN, Ariaens A, Postma FR, Varnai P, Balla T, Divecha N,**

609   **Jalink K, and Moolenaar WH.** Regulation of connexin43 gap junctional communication by

610   phosphatidylinositol 4,5-bisphosphate. *J Cell Biol* 177: 881-891, 2007.

611   51.   **Wang CM, Lincoln J, Cook JE, and Becker DL.** Abnormal connexin expression underlies

612   delayed wound healing in diabetic skin. *Diabetes* 56: 2809-2817, 2007.

613   52.   **Wang HX, Gillio-Meina C, Chen S, Gong XQ, Li TY, Bai D, and Kidder GM.** The canonical

614   WNT2 pathway and FSH interact to regulate gap junction assembly in mouse granulosa cells. *Biol*

615   *Reprod* 89: 39, 2013.

616   53.   **Wang Q, Symes AJ, Kane CA, Freeman A, Nariculam J, Munson P, Thrasivoulou C, Masters**

617   **JR, and Ahmed A.** A novel role for wnt/ca signaling in actin cytoskeleton remodeling and cell motility

618   in prostate cancer. *PLoS ONE* 5: e10456, 2010.

619   54.   **Whyte JL, Smith AA, Liu B, Manzano WR, Evans ND, Dhamdhere GR, Fang MY, Chang HY,**

620   **Oro AE, and Helms JA.** Augmenting endogenous Wnt signaling improves skin wound healing.

621   *PLoSOne* 8: e76883, 2013.

622   55.   **Xia X, Batra N, Shi Q, Bonewald LF, Sprague E, and Jiang JX.** Prostaglandin promotion of

623   osteocyte gap junction function through transcriptional regulation of connexin 43 by glycogen

624   synthase kinase 3/beta-catenin signaling. *Mol Cell Biol* 30: 206-219, 2010.

625   56.   **Xie H, Cui Y, Hou S, Wang J, Miao J, Deng F, and Feng J.** Evaluation of Connexin 43

626   Redistribution and Endocytosis in Astrocytes Subjected to Ischemia/Reperfusion or Oxygen-Glucose

627   Deprivation and Reoxygenation. *BioMed research international* 2017: 5064683, 2017.

628 57.   **Zhao X, Tang X, Ma T, Ding M, Bian L, Chen D, Li Y, Wang L, Zhuang Y, Xie M, and Yang D.**

629 Levonorgestrel Inhibits Human Endometrial Cell Proliferation through the Upregulation of Gap

630 Junctional Intercellular Communication via the Nuclear Translocation of Ser255 Phosphorylated

631 Cx43. *BioMed research international* 2015: 758684, 2015.

632 58.   **Zhou JZ and Jiang JX.** Gap junction and hemichannel-independent actions of connexins on

633 cell and tissue functions--an update. *FEBS letters* 588: 1186-1192, 2014.

634 **Figure Legends**

635 Figure1

636 Translocation of β-catenin (red) and Cx43 (green) to the nucleus (counterstained with DAPI, blue) in

637 response to activation by Wnt ligands (200ng/ml) in PC3 cell line using immunocytochemistry.

638 Control vehicle treated (A, D) or after activation with Wnt5A (B, E) and Wnt9B (C, F). *Inset*: shows the

639 larger field from which the higher magnification images were taken. Z-stacks were obtained using a

640 Leica SPE confocal microscope. Wnt activation increases the translocation of both ß-catenin (red)

641 and Cx43 (green) translocation towards the nucleus. Representative images of three individual

642 experiments are shown. Scale bar= 10µm.

643

644 Figure 2

645 Translocation of Cx43 to the nucleus in response to Wnt ligands (200ng/ml) in PC3 cell line, control

646 (A) or after activation with Wnt5A (B) and Wnt9B (C). PC3 cells were grown on coverslips, treated

647 with Wnt ligands, fixed, and stained for Cx43 EM investigation. Representative images obtained

648 using a TEM microscope are shown; white dotted lines demarcate the nuclear boundary; white

649 arrows indicate some of the Cx43 labelled electron dense puncta; purple arrows indicate putative

650 Cx43 hemi-channels. *Inset*: High-magnification images of the nuclear region. Scale bar, 2µm.

651 Between 18–25 cells were analyzed and box plots show calculated Cx43 level/nucleus (D); there was

652 a significant (***p<0.0001) increase in the Cx43 signal in the nuclei of cells treated with Wnt (5A, box

653 shaded green and 9B, box shaded blue) compared to vehicle control (box shaded yellow). The

654 distribution of calculated Cx43 expression (data binned) on the cell membrane (green), in the cytosol

655 (red) and nucleus (purple) separately in response to activation by Wnt ligands (200ng/ml) in PC3

656 cells (E-G). Cells were analyzed from EM images of control (E) or after activation with Wnt5A (F) and

657 Wnt9B (G) were analyzed as described under "Experimental Procedures." Activation of Wnt signaling

658 results in the re-distribution of Cx43 signal as follows: 5-10, 10-20 and 50-60 in the cell membrane,

659 cytosol and nucleus, respectively. Box plot of calculated Cx43 (H) and β-catenin (I) expression,

660 represented by mean count of electron dense puncta, on the cell membrane (box border:

661 blue/green), in the cytosol (box border: pink) and nucleus (box border: purple) in untreated controls

662 (box fill: orange) and in response to activation by Wnt (200ng/ml) 5A (box fill: green) and 9B (box fill:

663 blue) in PC3 prostate cancer cell line. Images were obtained using a TEM microscope similar to those

664 used in e.g. Figs 2 and 7. Cx43 (H) expression was reduced in the membrane and cytosol, increased in

665 nucleus, significantly for Wnt-treated compared to control cells. The expression of β-catenin (I) in

666 cytosol and nucleus increased significantly for Wnt-treated versus control cells; 25 cells from 3

667 independent experiments were analyzed. Mann-Whitney U test was used to measure the

668 significance of difference between control and Wnt treated cells is annotated (ns = not significantly

669 different; *$p<0.05$; **$p<0.01$;***$p<0.0001$).

670

671 Figure 3

672 Cx43 and β-catenin translocation to the nucleus in response to activation by Wnt ligands (200ng/ml)

673 in Cx43c PC3 prostate cancer cell lines, control (A, D) or after activation with Wnt5A (B, E) and

674 Wnt9B (C, F); Cx43 expression was decreased in Cx43kd cells, control (G) or after Wnt5A (H) or 9B

675 treatment (I), as would be expected, and more β-catenin translocation were observed in Cx43kd

676 cells, control (J) or after activation with Wnt5A (K) and Wnt9B (L). Cells were grown in eight-well

677 chamber slides, treated with Wnt ligands, fixed, and stained for β-catenin (red), Cx43 (green) and

678 nucleus (blue). Representative images from three independent experiments are shown as Z-stacks

679 obtained using a Leica SPE confocal microscope. Scale bar, 10μm.

680   Figure 4

681   Co-localization of ß-catenin or Cx43 with DAPI (nuclear counterstain) in wild type and knock-down

682   cells

683   (A) Box plots of calculated Pearson coefficient for β-catenin co-localization in the nucleus in Cx43c

684   and Cx43kd PC3 cells. Immunohistochemistry and image analysis was performed as described under

685   "Experimental Procedures". Cy3 (label for β-catenin) showed significantly increased co-localization

686   coefficients with DAPI (nuclear counterstain) for Wnt-treated (200 ng/ml) versus control cells in both

687   Cx43c and Cx43kd cells (at least *p<0.05). Co-localization coefficients of β-catenin was significantly

688   increased in Cx43kd cells compared with Cx43c cells (§ p<0.0002) and between vehicle treated

689   controls and Wnt (5A or 9B) treated cells (asterisks, *p<0.05*** p <0.001) within Cx43c (hollow bars)

690   and Cx43kd cells (shaded bars), respectively (n= 49-106 cells for each condition from 2-3

691   independent experiments).

692   (B) Box plots of calculated Pearson coefficient for β-catenin co-localization in the nucleus in Cx43c

693   and Cx43kd 3T3 cells. Immunohistochemistry and image analysis was performed as described under

694   "Experimental Procedures". Cy3 (label for β-catenin) showed significantly increased co-localization

695   coefficients with DAPI (nuclear counterstain) for Wnt-treated (200 ng/ml) versus control cells in both

696   Cx43c and Cx43kd cells (p<0.05). Co-localization coefficients of β-catenin was significantly increased

697   in Cx43kd cells compared with Cx43c cells (§ p<0.02) and between vehicle treated controls and Wnt

698   (5A or 9B) treated cells (asterisks *p <0.05 and ** p <0.01) within Cx43c (hollow bars) and Cx43kd

699   cells (shaded bars), respectively (n = 32-172 cells from 2-3 independent experiments).

700   (C) Box plots for the calculated Pearson co-localization coefficient of β-catenin and nuclear

701   counterstain DAPI indicating ß-catenin translocation into the nucleus in CTNNB1c (wild type, hollow

702   bars), CTNNB1sc (scramble shRNA control, hatched bars) and CTNNB1kd (Cx43 knockdown, shaded

703   bars) PC3 cells. Immunohistochemistry and image analysis was performed as described under

704   "Experimental Procedures" and between 16-144 cells for each conditions from 2-3 independent

705   experiments were analyzed. There was no significant difference in the co-localization coefficients of

706   ß-catenin between control, CTNNB1c (hollow gray bar) and CTNNB1sc (hatched gray bar). Co-

707   localization coefficient for β-catenin was significantly (asterisks *$p<0.05$, *** $p<0.001$) increased in

708   Wnt treated CTNNB1c (hollow, 5A green, 9B blue) and CTNNB1sc (hatched, 5A green, 9B blue),

709   compared to their respective control, vehicle treated, cells.

710   Figure 5

711   TEM of Cx43 and β-catenin translocation to the nucleus in response to activation by Wnt ligands

712   (200ng/ml) in Cx43c (vector only control) and Cx43kd (shRNA knockdown) PC3 cells. Cx43 protein

713   expression was measured in vehicle only (A,D) or after activation with Wnt5A (B,E) and Wnt9B (C,F)

714   in Cx43c and Cx43kd cells, respectively. There was a significant increase in puncta/nucleus in Wnt

715   treated Cx43c cells compared to vehicle controls (**, $p<0.001$). There was no statistically significant

716   difference in the Cx43 positive puncta/nucleus between vehicle treated or Wnt treated Cx43kd cells

717   (G). Similar to fluorescence immunohistochemistry results, there was a significant increase in the

718   translocation of ß-catenin protein into the nucleus in Wnt treated cells (I,J) compared to vehicle

719   control (H) Cx43c cells using TEM. Measurement of the expression of ß-catenin protein (N) also

720   showed that significantly (section, § $p<0.001$) more β-catenin-positive puncta were translocated to

721   the nucleus in Cx43kd cells (K), compared to Cx43c cells (H); There was also a significant (star ★

722    $p<0.001$) increase in ß-catenin expression in Wnt5A treated compared to vehicle control in Cx43kd

723   cells (L); there was no significant difference in vehicle control vs Wnt 9B treated Cx43kd cells (M). A

724   quantitation of ß-catenin protein expression in Cx43c and Cx43kd cells is given in (N). *Inset*: shows

725   the larger field from which the higher magnification images were taken. Scale bar, 2µm. EM image

726   analysis was performed as described under "Experimental Procedures." Between 17-38 cells from 3

727   independent experiments were analyzed and box plots show calculated number of electron dense

728   puncta of Cx43 (G) or β-catenin (N) per nucleus.

729   Figure 6

730   Immunocytochemical analysis of β-catenin (red) and Cx43 (green) translocation to the nucleus (blue)

731   in response to activation by Wnt ligands (200ng/ml) in CTNNB1c and CTNNB1sc PC3 prostate cancer

732   cell line, vehicle control (A, D,G, J) or after activation with Wnt5A (B,E,H,K) and Wnt9B (C,F,I,L); more

733   Cx43 translocation was observed in CTNNB1kd cells, control (P) or after activation with Wnt5A (Q)

734   and Wnt9B (R). ß-catenin expression was decreased in CTNNB1kd cells (M), this was also the case

735   even after Wnt treatment (N and O). Cells were grown in eight-well chamber slides, treated with

736   Wnt ligands, fixed, and stained for β-catenin, Cx43 and nucleus using immunocytochemistry

737   protocols described under "Experimental Procedures". Z-stacks obtained using a Leica SPE confocal

738   microscope are shown. Representative images of three individual experiments are shown. Scale bar

739   = 10μm.

740   Figure 7

741   Translocation of Cx43 to the nucleus in response to activation by Wnt ligands (200ng/ml) in

742   CTNNB1c and CTNNB1sc PC3 cells line using TEM. Vehicle treated, control (A, D) or after activation

743   with Wnt5A (B, E) and Wnt9B (C, F). Increased Cx43 translocation was observed in CTNNB1kd cells,

744   control (G) or after activation with Wnt5A (H) and Wnt9B (I) compared to Wnt treated CTNNB1c and

745   CTNNB1sc. Between 20-76 cells from 2-3 independent experiments were analyzed. Representative

746   images of three individual experiments are shown. Scale bar = 2μm.

747

748   Figure 8

749   β-catenin, Cx43 and CK1δ interact with each other in PC3 cells. (A) Immunoblot/co-IP analysis of the

750   native CK1δ complex from whole-cell PC3 lysates using antibody indicated at the left of each panel.

751   Both β-catenin and Cx43 were detected in native CK1δ complexes from PC3 cells. (B)

752   Immunoblot/co-IP analysis of the native Cx43 complex from whole-cell PC3 lysates using antibody

753   indicated at the left of each panel. Both β-catenin and CK1δ were detected in Cx43 complexes from

754   PC3 cells. The IP antibodies were used with CK1δ (4μg; sc-20709; Santa Cruz Biotechnology) and

755   Cx43 (4ug; C6219, Sigma). The primary antibodies for Western blot were used with β-catenin (1:500;

756   ab22656, Abcam), CK1δ (1:200; sc-55553, Santa Cruz Biotechnology) and Cx43 (1:4000; C8093,

757   Sigma). The secondary antibodies were used with goat anti-mouse IgG-HRP (1:2000; sc-2005, Santa

758   Cruz Biotechnology) and Goat F(ab')2 Anti-Mouse IgM mu chain-HRP (1:2000; ab5930, Abcam).

759   Lanes are numbered 1, 2 and 3 for input, CKIδ and IgG, respectively; MW indicates the molecular

760   weight marker lane. A representative of 3 independent experiments is shown.

761   Figure 9

762   Re-epithelialization rates (straight-line measurement from wound edge to distal tongue of re-

763   epithelization into the wound-bed) following injury in control and Wnts treated rat skin epidermis.

764   Images show examples of re-epithelialization in rat skin epidermis rates at 1 day post-wounding

765   (dpw), control (A), Wnt5A (B), and Wnt9B (C) treated; and at 3 day post-wounding, control (D),

766   Wnt5A (E), and Wnt9B (F) treated. White dotted lines indicate the dermal-epidermal border of re-

767   epithelialization. (G) Box plot (shaded yellow for vehicle control, green for Wnt5A and blue for

768   Wnt9B treated animals; n=8 for Wnt treated rats and n=5 for control at 1 and 3 dpw) showing the

769   rate of re-epithelialization was significantly (** p<0.02) increased relative to controls in Wnt treated

770   rats at 1 day post-wounding (dpw, brown outlined box). The rate of re-epithelialization was similar

771   relative to controls in Wnt treated rats at 3 day post-wounding (gray outlined box).

772

773   Figure 10

774   A model for Wnt signaling pathway that regulates ß-catenin and Cx43 in mammalian cell lines (only

775   the cell membrane and the nucleus shown in the schematic for clarity). Proposed steps of Wnt

776   signaling in mammalian cells are as follows: binding of Wnts (1) results in the activation of

777   intracellular calcium stores (2) that increase in the intracellular concentration of free calcium (3). The

778   increase in free calcium depolarizes the cell membrane and as calcium enters the nucleus (4), the

779   nuclear envelope (NE) is depolarized (48); the activation of Wnt/Ca2+ pathway also increases (5)

780   Ca2+/calmodulin-dependent kinase (CamKII) activity (53). It is well established by previous studies

781   (29) (that activation of Wnt signaling (6) desequesters the caged β-catenin (β-cat) that is

782   phosphorylated (P) and ubiquitinated (UUU) prior to degradation in proteasomes, gray square) in

783   the cytosol. The desequestered β-catenin (7) translocation is facilitated across the NE, which is now

784   depolarized (8) and has increased nucleoplasmic calcium (9). Cx43 and β-catenin are partly

785   colocalized at the cell membrane (39). Cx43 is a likely partner in the ß-catenin destruction complex.

786   The membrane and cytosolic Cx43 are moving with ß-catenin concomitantly and largely translocated

787   into the nucleus subsequent to Wnts signaling activation. β-catenin and Cx43 are co-localized in the

788   nucleus where β-catenin binds to LEF/TCF proteins to initiate gene transcription and Cx43 is a likely

789   co-transcription factor. For simplification, many other proteins involved in Wnt signaling are not

790   shown and multiple other pathways such as Wnt/PCP pathways are not included in the illustration.

791   The steps for which evidence is given in the manuscript are shown with arrows shaded purple.

792

793   Supplemental Figure 1

794   Confocal images of simultaneous detection of ß-catenin and Cx43 translocation to the nucleus in

795   response to activation by Wnt 10B in PC3 prostate cancer cell line. Cells were grown in eight-well

796   chamber slides and wells were either treated with Wnt 10B (200ng/ml) or with PBS (control) –

797   manual staining was performed using primary (see methods) and appropriate secondary fluorophore

798   labelled antibodies. A to D are individual channels for (A) DAPI, nuclear stain (blue), (B) Cx43 (green)

799   and (C)ß-catenin (red); D is a composite image of all the channels. Images E to H are for Wnt 10B

800   treated cells; individual channels for (E) DAPI, nuclear stain (blue), (f) Cx43 (green) and (G)ß-catenin

801   (red); H is a composite image of all the channels. Individual Z-stacks were obtained using a Leica SPE

802   confocal microscope are shown. Representative images of three individual experiments are shown.

803   Scale bar = 10µm.

804   Supplemental Figure S2

805   Confocal images of Cx43 translocation to the nucleus in response to activation by Wnt ligands

806   (200ng/ml) in 3T3 fibroblast cell line, in control (A) and Wnt 9B treated cells (B). Cells were grown in

807   eight-well chamber slides, treated with Wnt ligands, fixed, and stained for Cx43 (green) and nucleus

808   (counterstained with DAPI, blue) using protocols described under "Experimental Procedures." Z-

809   stacks obtained using a Leica SPE confocal microscope are shown. Representative images of three

810   individual experiments are shown. Scale bar = 10µm.

811   Supplemental Figure S3

812   A representative Western blot (n=3) from two independent cell fractionation experiments of PC3

813   cells with and without (A) Wnt 5A and (B) Wnt 9B treatment. Each lane of the gel was loaded with 12

814   µg of fractionated protein (untreated and treated, respectively – see methods below): cytosolic

815   (Cytosol, lanes 2 and 3), cell membrane (Cell Memb., lanes 5 and 6) and nuclear (Nuclear, lanes 8

816   and 9); lanes 1, 4, 7 and 10 were loaded with Precision Plus Protein Dual Color Standards (Bio Rad).

817   The PVDF membranes were cut into two strips of 250 to 50 kDa and 50 to 10 kDa and incubated with

818   anti-Lamin A (expected size ~70k Da), a marker for the nuclear fraction, and anti-Cx43 (expected size

819   ~41-43k Da) antibodies (both shown in black boxes), respectively. The 50 to 10kDa blot was

820   'stripped' (shown in a blue box) and further probed with ß-actin (expected size ~42k Da).

821   Cell fractionation was performed using Qproteome cell compartment kit (Qiagen) according to

822   manufacturer's protocol. Briefly, PC3 cells were grown in 25ml flasks and treated with Wnt5A and

823   Wnt9B in PBS (1.5ml) at 37°C as described in methods; vehicle treated PC3 cells were used as

824   controls. The cell were lysed and fractionated into cytosolic (Cytosol), cell membrane (Cell Memb.)

825   and nuclear (Nuclear) fractions using the Qproteome (Qiagen) followed by protein quantitation using

826   Pierce BCA protein assay kit (Thermo Fisher Scientific); 12 µg protein for each fraction was loaded

827   onto gels and resolved on Precast Gels (Bio Rad)using Mini-PROTEAN (Bio Rad) system. The resolved

828   proteins were transferred onto a PVDF membrane using Trans-Blot® TurboTM Blotting System (Bio

829   Rad). The PVDF membranes were cut into two strips of 250 to 50 kDa and 50 to 10 kDa and

830   incubated with anti-Lamin A (cat no. L1238, Sigma, at 1:5000 dilution), a marker for the nuclear

831   fraction, and anti-Cx43 (C6219, Sigma, at 1:8000 dilution, expected size ~41-43k Da) antibodies,

832   respectively for over-night at 4°C. Following this, the PVDF membranes were washed and probed

833   with appropriate Horse Radish Peroxidase (HRP) conjugated secondary antibodies (Peroxidase

834   AffiniPure Donkey Anti-Rabbit IgG (H+L), dilution 1:10000, Jackson ImmunoResearch Laboratories,

835   Inc) for 120 min at RT. The HRP signal was detected using Bio Rad Clarity Western Enhanced Chemi-

836   luminescence (ECL) substrate and blots were imaged using Chemi Doc (Bio Rad) system. Dual colored

837   standard protein markers (Bio Rad Precision Plus Protein, Bio Rad) were used which are recognized

838   by the Chemi Doc system. ß-actin, a 42 kDa ubiquitous protein, a commonly used as a protein

839   loading control was also used. To detect ß-actin the 50 to 10 kDa PVDF membrane strip (see above)

840   was 'stripped' using Thermo Scientific Restore PLUS Western Blot Stripping Buffer (Ref: 46430) using

841   standard protocols and incubated with anti-ß-actin antibody (ab6276, Abcam, at 1:5000 dilution,

842   expected size ~42k Da). Subsequent to detection with an HRP secondary antibody (Peroxidase

843   AffiniPure Donkey Anti-Mouse IgG (H+L), Jackson ImmunoResearch Laboratories, Inc), the HRP signal

844   was detected as described earlier.

845

846   Supplemental Figure S4

847   Western blots to confirm knockdown of Cx43 and ß-catenin using Tubulin (Tub) was included as

848   loading control.

849   (A) Cx43 expression in control and Cx43 knockdown cells measured by Western blotting in Cx43c and

850   Cx43kd in PC3 cells (representative blots on top and quantified data underneath). Cx43 level was

851   significantly reduced in Cx43kd cells compared with Cx43c cells. Quantitation of the signal shows

852   that Cx43 protein levels were knocked down in Cx43kd PC3 cells compared to Cx43c cells (* $p<0.05$;

853   n = 3).

854   (B) ß-catenin expression in control and Cx43 knockdown cells measured by Western blotting.

855   Knockdown of Cx43 did not change the expression levels of β-catenin in PC3 cells. β-catenin levels

856   were analyzed by Western blot in Cx43c and Cx43kd PC3 prostate cancer cell lines. Quantitation of

857   the signal shows that knockdown of Cx43 did not change the expression levels of β-catenin.

858   (C) Anti-β-catenin antibody on PC3 cells; vector only control (CTNNB1c), scrambled shRNA control

859   (CTNNB1sc) and short-hairpin RNA to knockdown ß-catenin expression (CTNNB1kd). ß-catenin levels

860   were significantly reduced in CTNNB1kd PC3 cells compared with CTNNB1c and CTNNB1sc cells.

861   Quantitation of the signal shows that β-catenin knockdown in CTNNB1kd PC3 cells compared to

862   CTNNB1c and CTNNB1sc cells (* indicates significant change in expression compared to control,

863    $p<0.05$; n = 3).

864   (D) Knockdown of β-catenin did not change the expression levels of Cx43 in PC3 cells using Western

865   blotting. Cx43 levels were measured in CTNNB1c, CTNNB1sc and CTNNB1kd PC3 prostate cancer cell

866   line. Quantitation of the signal shows that knockdown of β-catenin did not change the expression

867   levels of Cx43.

868

869   Supplemental Figure S5

870   Box plots of the rate of wound closure, in Cx43c (vector only, gray outlined box) and Cx43kd (Cx43

871   knockdown, brown outlined box) 3T3 fibroblast cells. Cells were wounded using WoundMaker

872   (Essen) and imaged for 48h at 2h interval. Cx43 knockdown accelerated the rate of cell migration

873   compared with Cx43c control cells (yellow shaded box, § p<0.001). Addition of Wnt5A (shaded

874   green) and Wnt 9B (shaded blue) accelerated the rate of wound closure in Cx43c cells compared to

875   vehicle treated controls (asterisks, **p<0.01;***p<0.001) but did not impact (ns, not significant)

876   upon the rate of wound closure in Cx43kd vehicle treated control cells compared to the respective

877   Wnt treated cells. Significance of difference between conditions was measured using the Mann

878   Whitney U test.

879   Supplemental data can be accessed at: https://figshare.com/s/1e0dcade1c40ab536ce9

880

881

882

883

884

Fig 1

ß-catenin   DAPI   Cx43

Fig 2

E

Control

Membrane
Cytosol
Nucleus

F

Wnt 5A

G

Wnt 9B

Count Cx43

Fig 2 contd

H

Box border key: Membrane Cytosol Nucleus

Count Cx43

Control   Wnt5A   Wnt9B

I

Count ß-catenin

Control   Wnt5A   Wnt9B

Fig 3

Fig 4

Fig 5

Control   **Wnt5A**   **Wnt9B**

Antibody : Cx43

Antibody : ß-catenin

Fig 6

Vehicle control　　+Wnt5A　　+Wnt9B

CTNNB1c

β-catenin

Cx43

CTNNB1sc

β-catenin

Cx43

CTNNB1kd

β-catenin
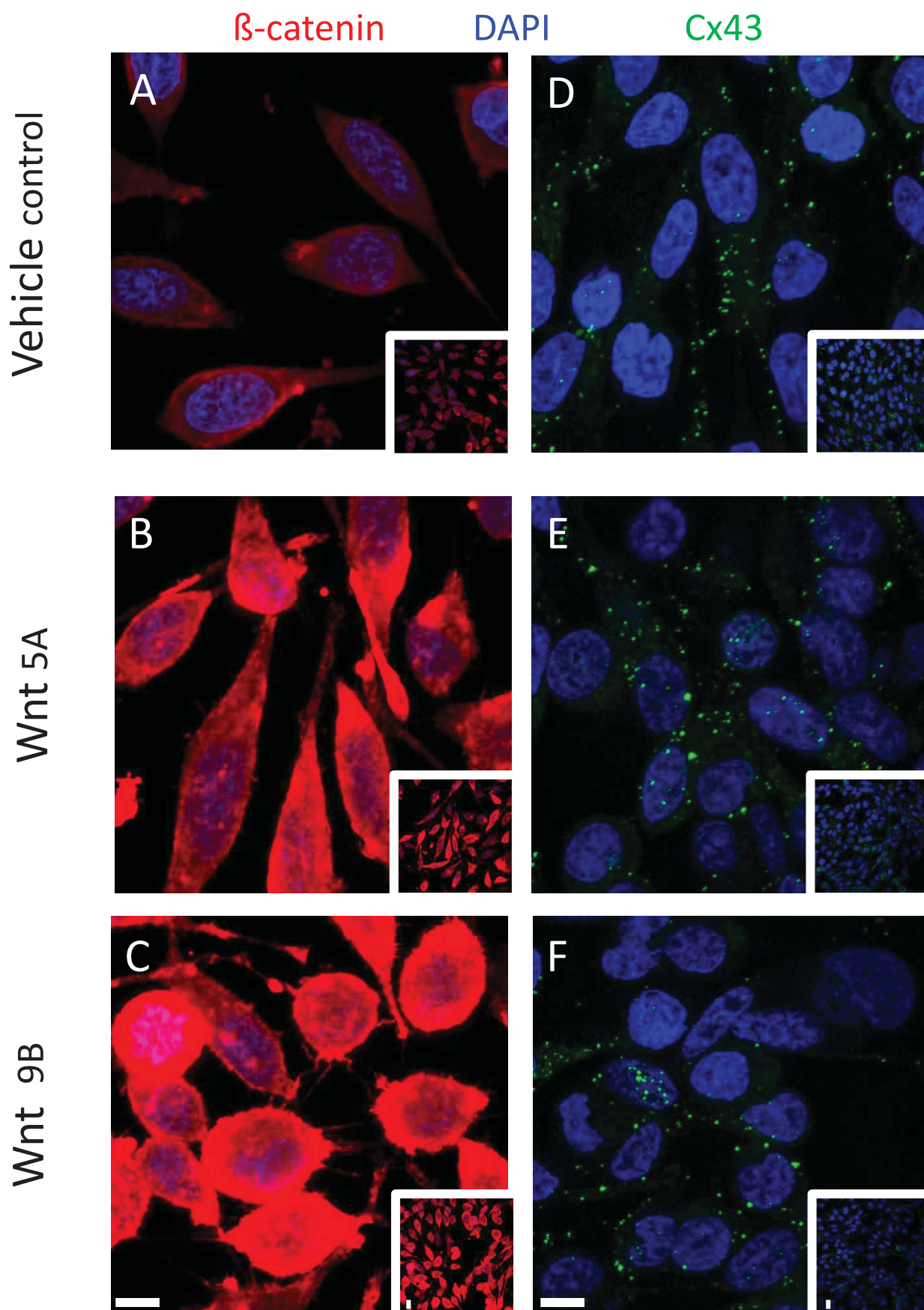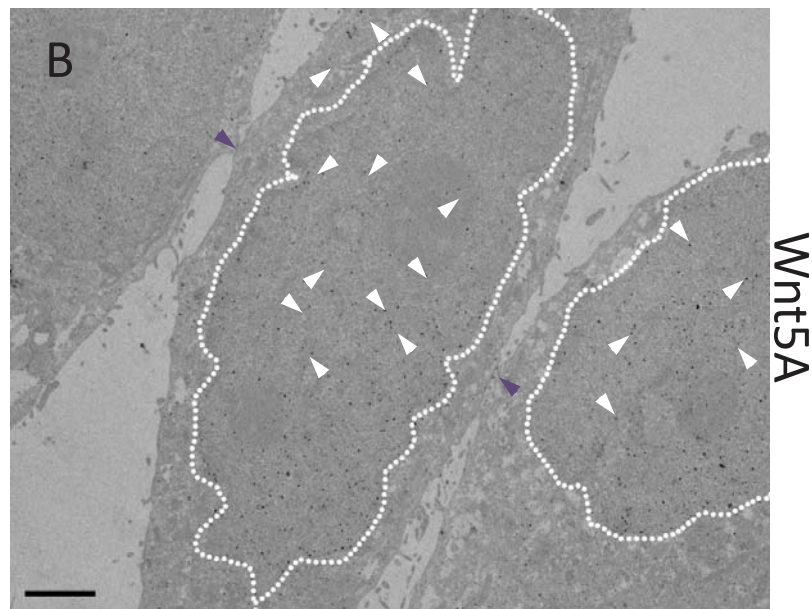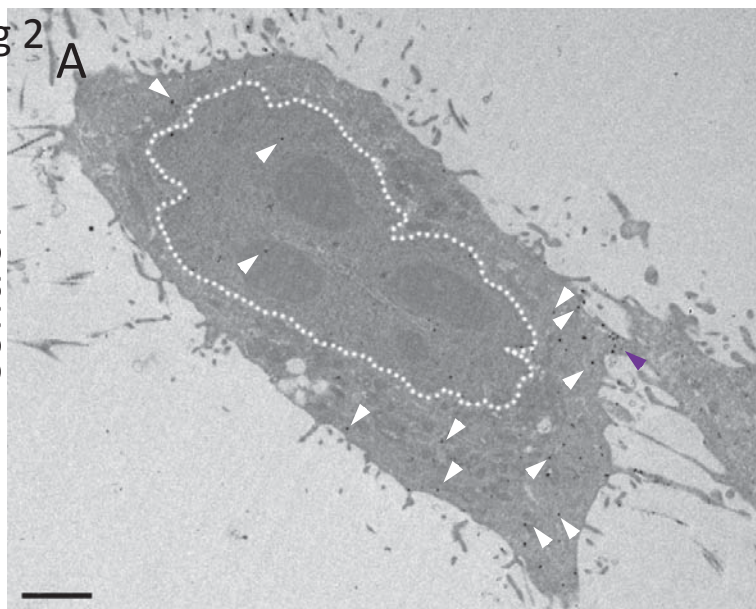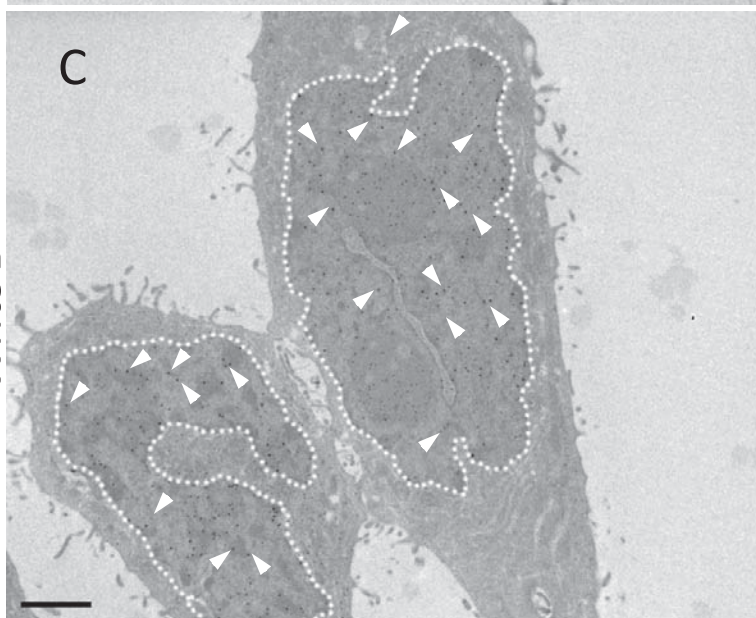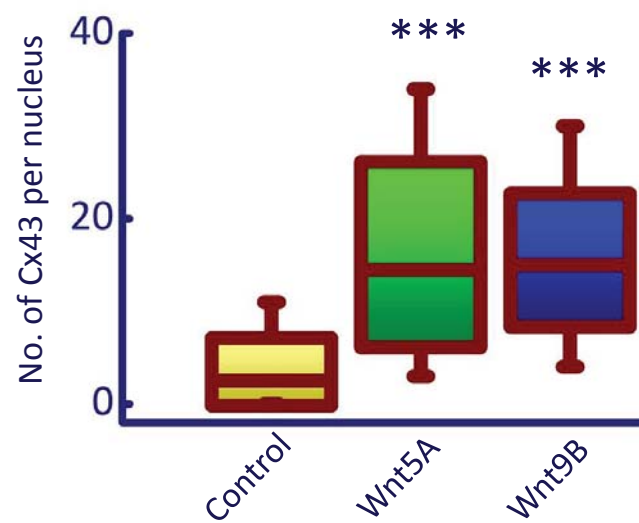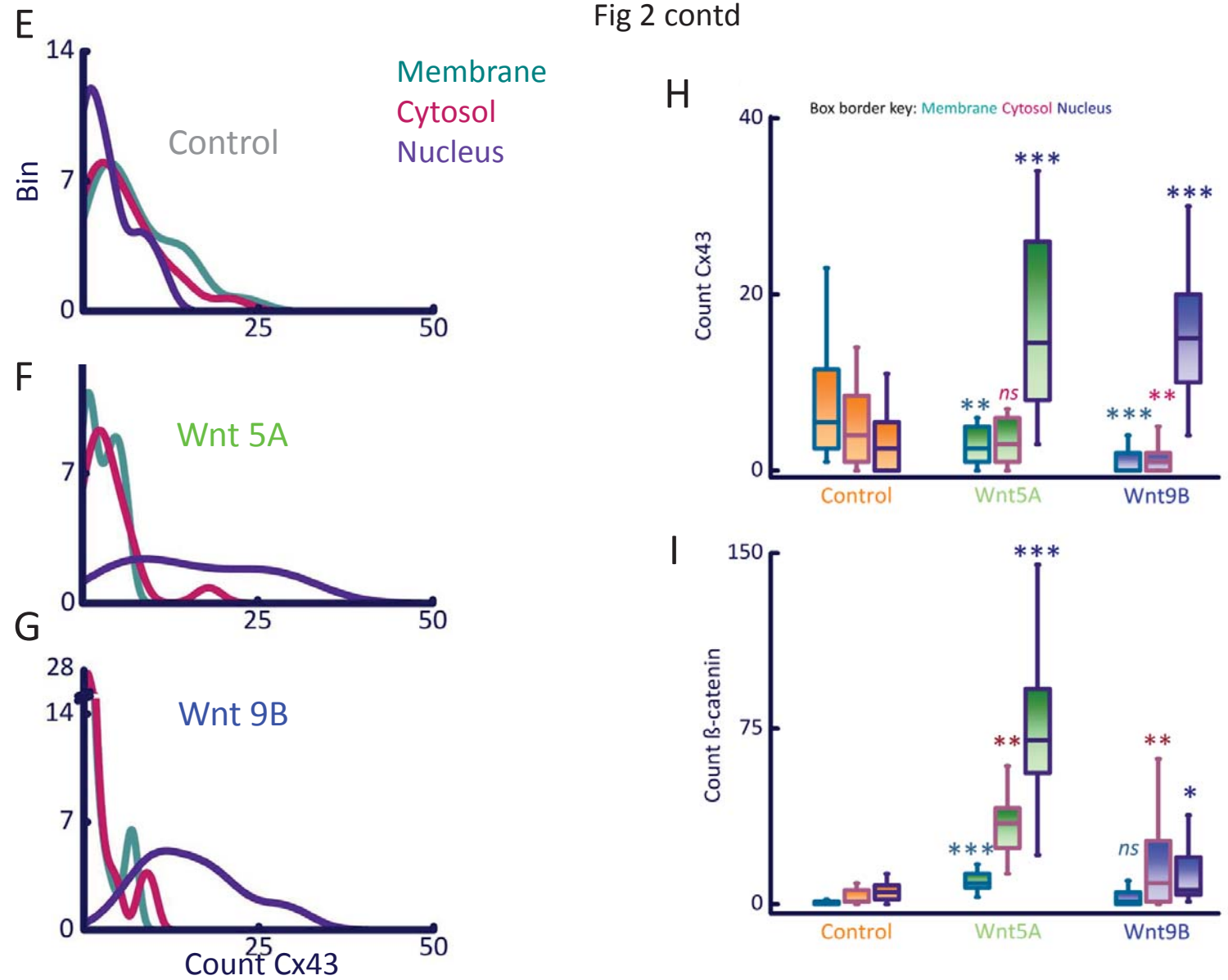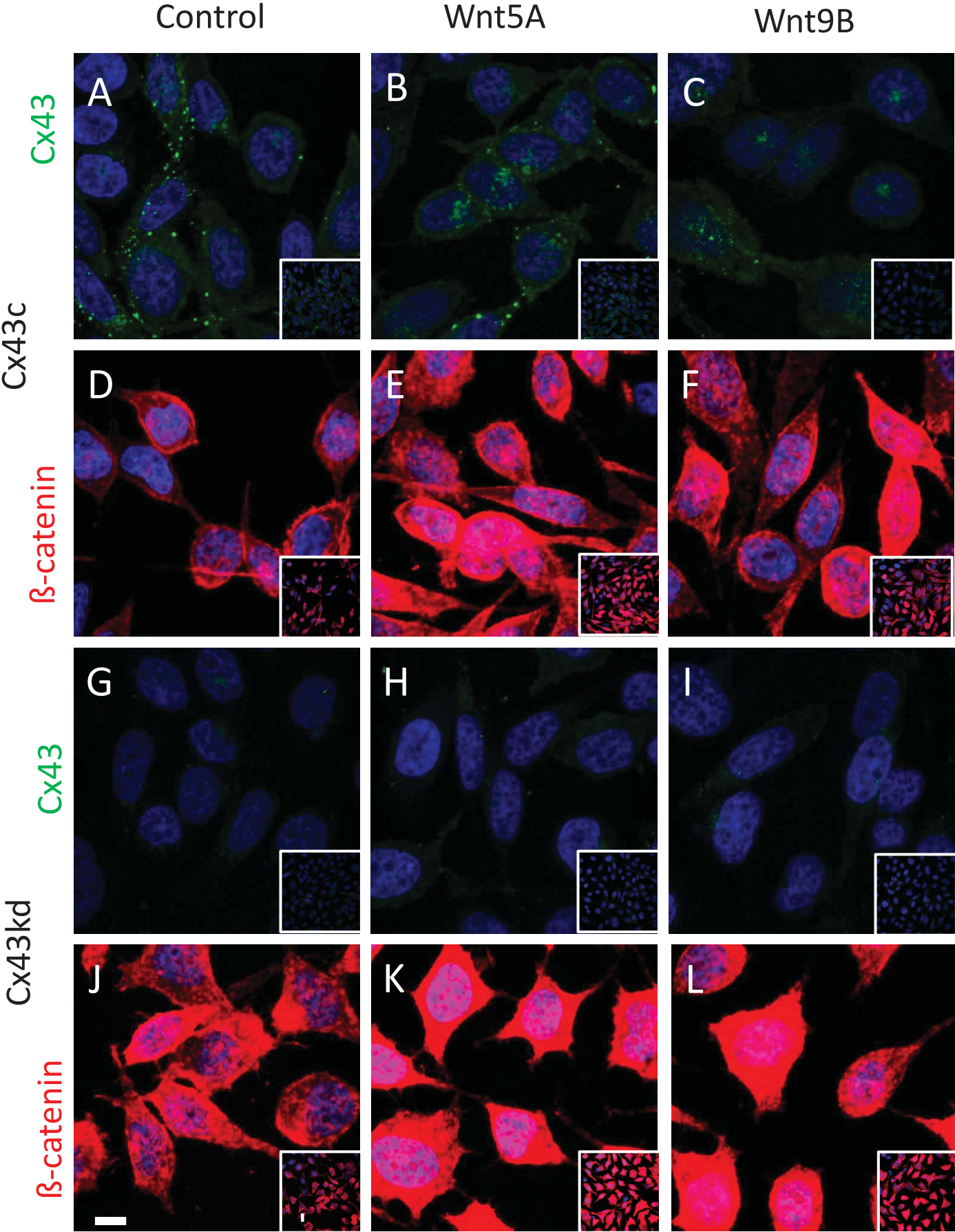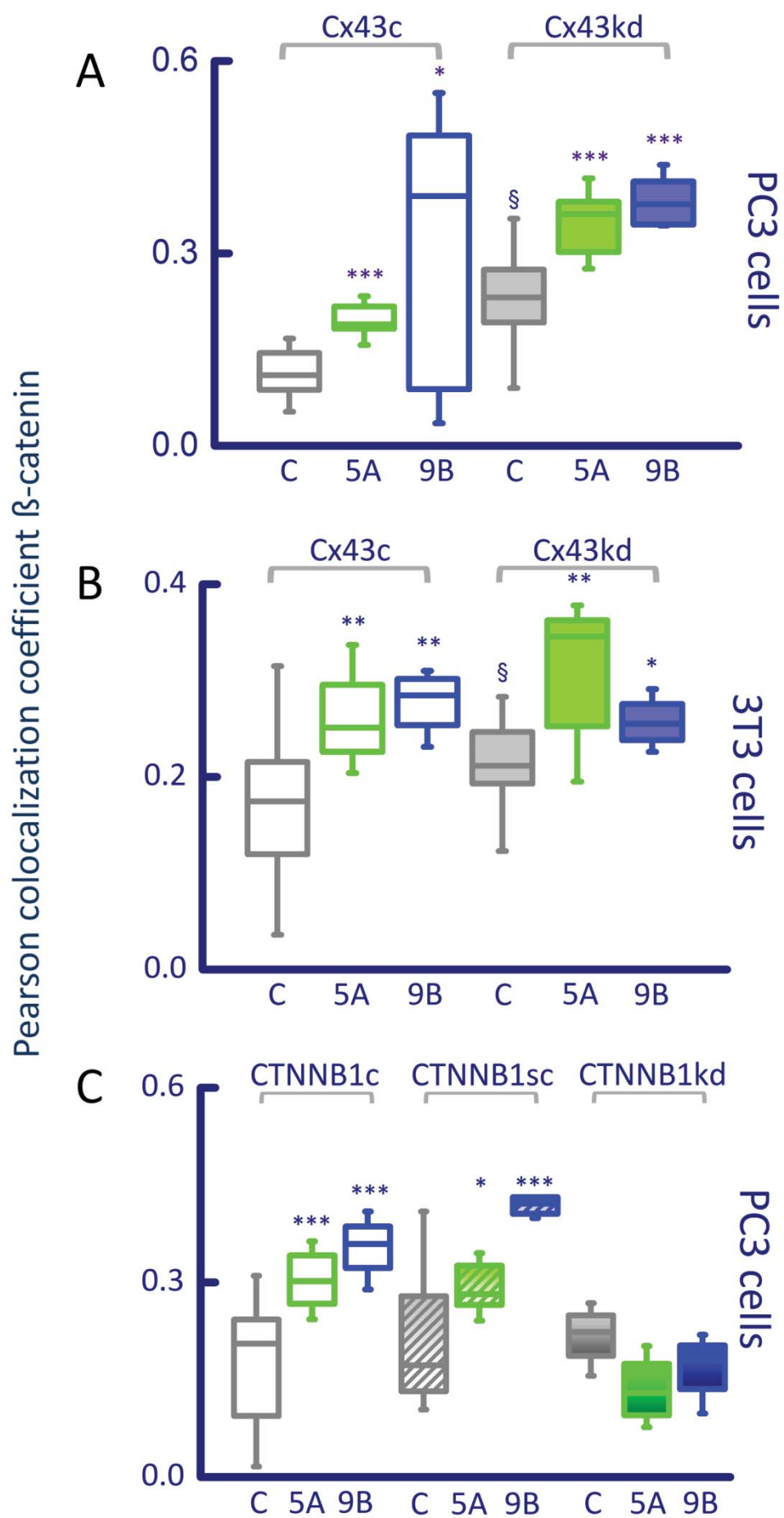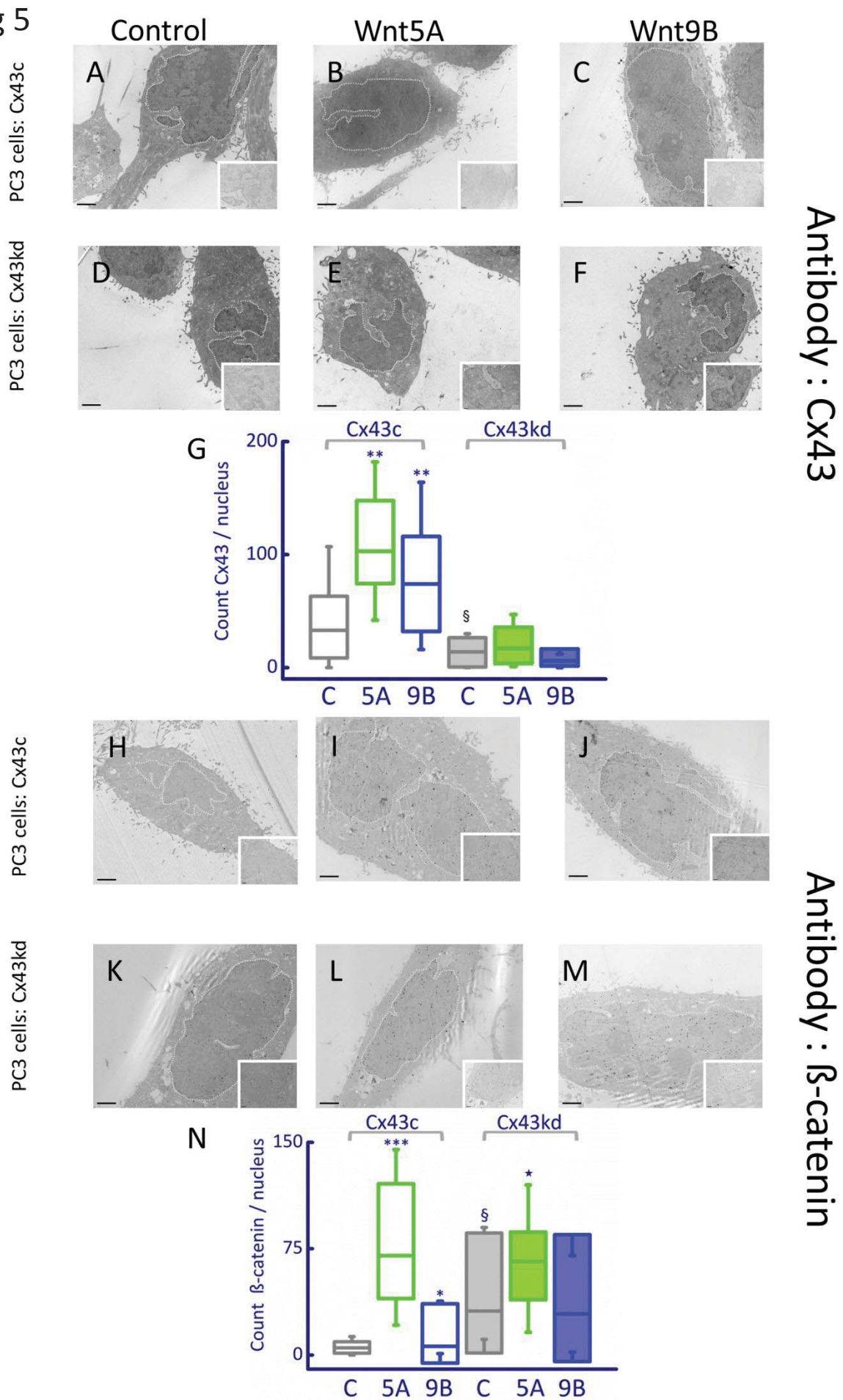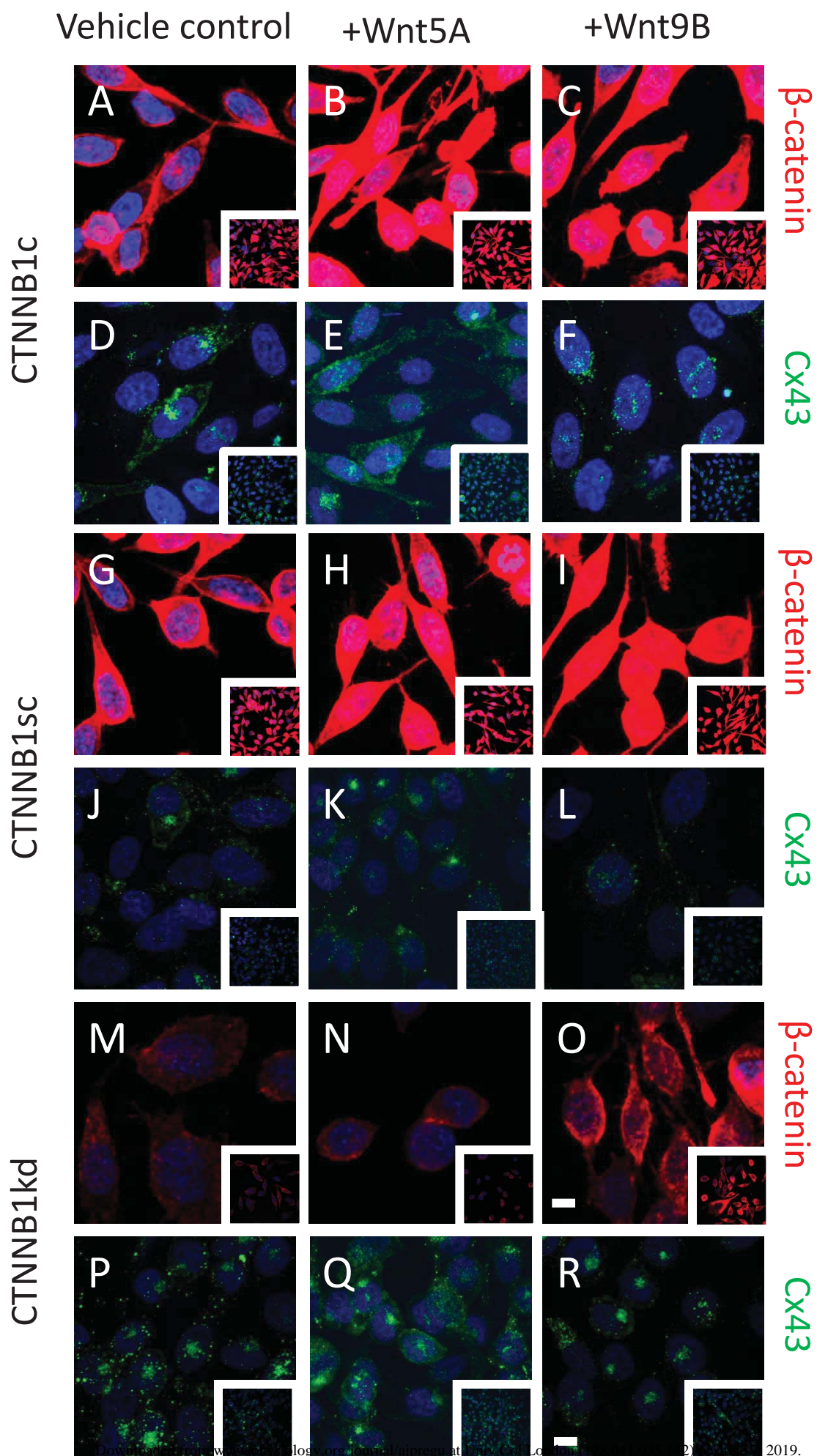
Cx43

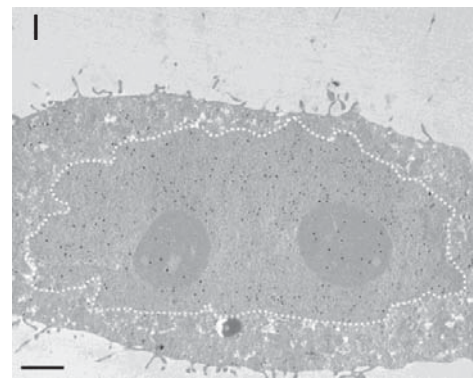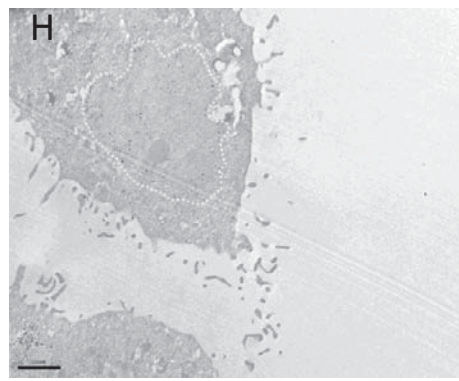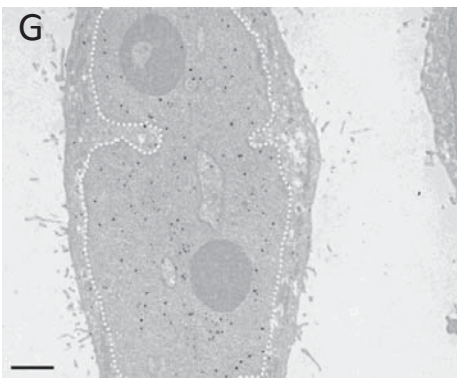Fig 7

Control   Wnt5A   Wnt9B
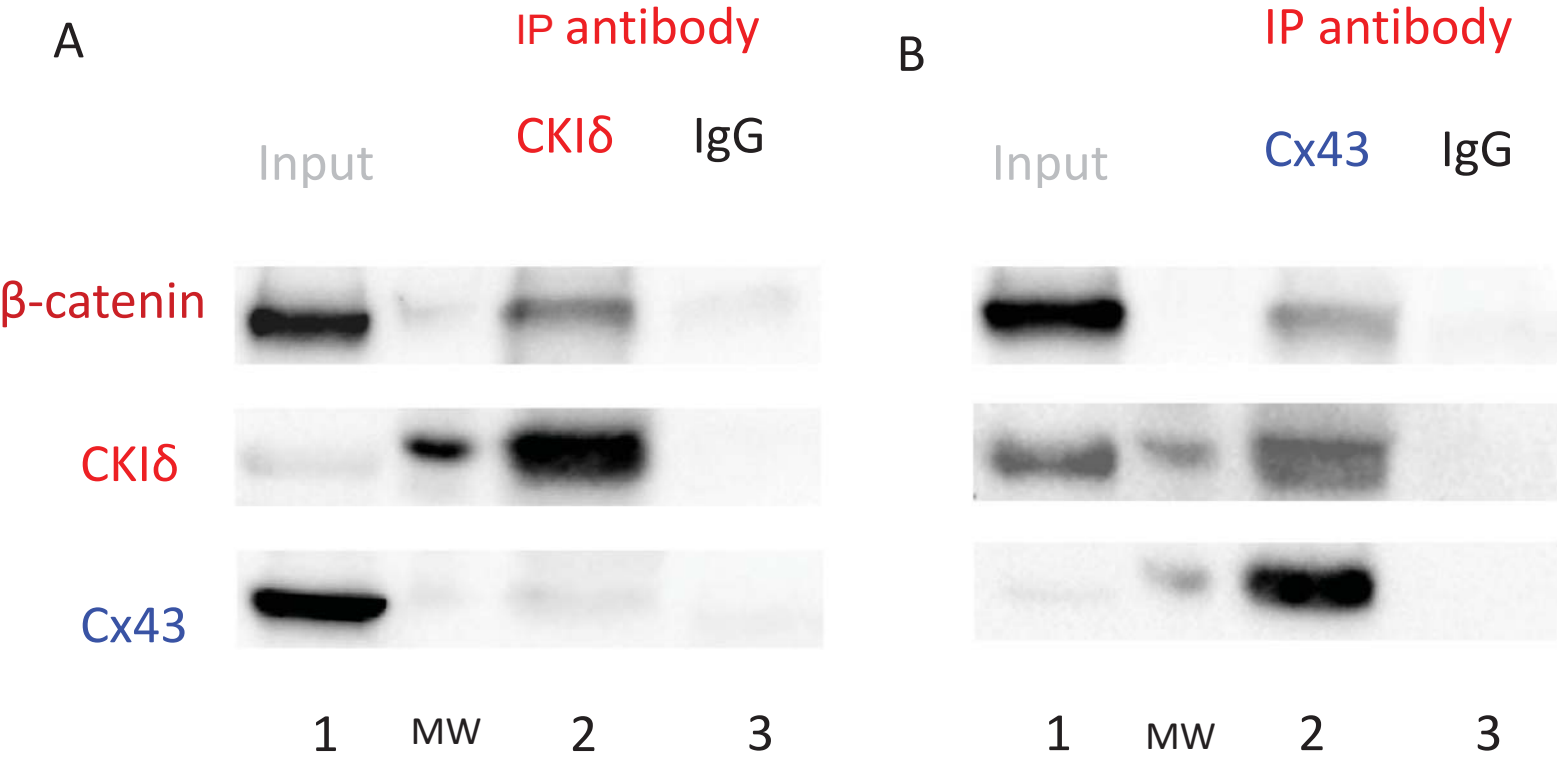
CTNBB1c
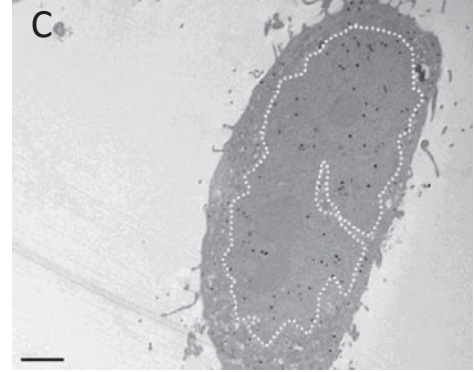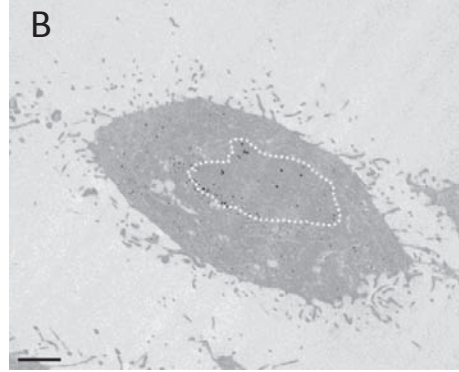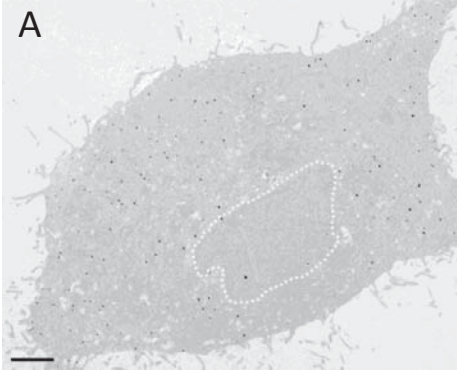
CTNBB1sc
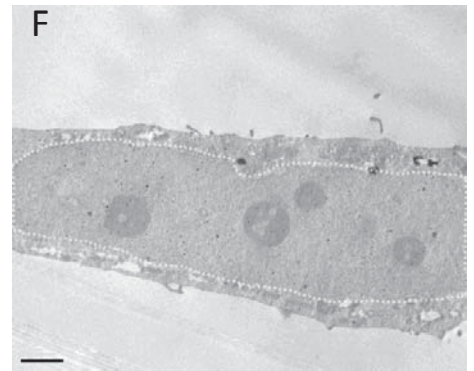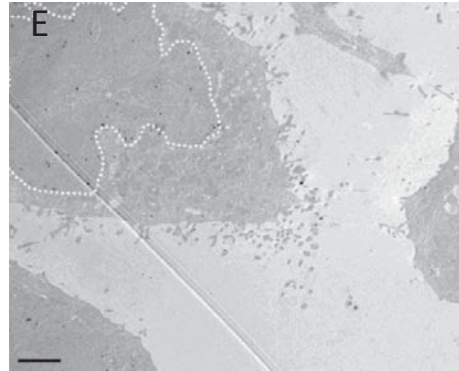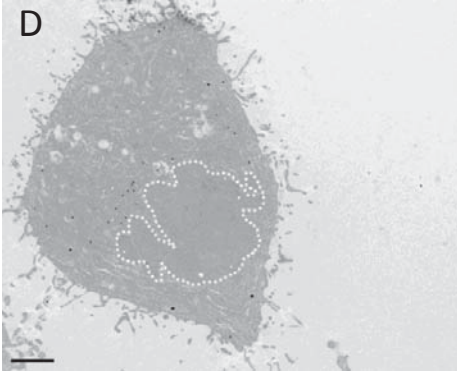
CTNBB1kd

PC3 cells - Cx43 antibody

Fig 8

A

IP antibody

β-catenin

CKIδ

Cx43

Input   CKIδ   IgG

1   MW   2   3

B

IP antibody

Input   Cx43   IgG

1   MW   2   3

Fig 9

Control   Wnt5A   Wnt9B

1dpw

3dpw

A   B   C

D   E   F

G

Re-epithelialization (μm)

1200

600

0

1dpw   3dpw

**   **

Control   5A   9B   Control   5A   9B

Fig 10